

# Evaluation of Cross-Flow Microfiltration Using a Dynamic Shear Enhanced Filtration System

## Master Thesis

Masterarbeit in der Studienrichtung  
Chemical and Pharmaceutical Engineering an der Technischen Universität Graz

submitted March 2014

Name: Claudia Payerl, BSc.

Adress: Glacisstraße 29

8010 Graz

Mat. No.: 0530594

<sup>1</sup>Research Center Pharmaceutical Engineering GmbH



## **Acknowledgement**

This work has been funded within the Austrian COMET Program under the auspices of the Austrian Federal Ministry of Transport, Innovation and Technology (bmvit), the Austrian Federal Ministry of Economy, Family and Youth (bmwfj) and by the State of Styria (Styrian Funding Agency SFG). COMET is managed by the Austrian Research Promotion Agency FFG.

Special thanks goes to the Novartis for their founding but also for the kind support throughout the project.

Personal I acknowledge the support from the RCPE laboratory staff who performed parts of the analytical measurements for this project.

Special thanks goes to my sister Linda, who encouraged me to finish this thesis and to my mother which stood behind me all the time.

Finally I want to thank all those people who supported me personally.

---

## Table of Content

1. Filtration.....	7
1.1. Microfiltration .....	7
1.2. Techniques in Microfiltration .....	10
1.2.1. Dead- End- Filtration .....	11
1.2.2. Cross- Flow- Filtration .....	15
1.2.3. Dynamic shear-enhanced membrane filtration .....	16
2. Theoretical Background.....	22
2.1. Mass Transfer Model and Concentration Polarization .....	23
2.1.1. Membrane fouling.....	27
2.2. Permeate flow-rate declaim .....	29
3. Quality by Design (QbD).....	33
3.1. QbD Implementation .....	34
3.2. Design of Experiment (DoE) .....	35
3.3. Analysis DynoTest Trials .....	37
3.4. Main DoE description .....	38
3.5. DoE Evaluation .....	42
4. Materials and Methods.....	44
4.1. Materials.....	44
4.2. DynoTest.....	47
4.2.1. DynoTest Principle Process Description .....	50
4.2.2. The control system of the DynoTest .....	51
4.2.3. The LabView control panel.....	52
5. Measurement Methods .....	54
6. Experimental Work .....	56
6.1 Preliminary Experiments.....	56
6.1.1. Feed Rate Calibration .....	56

---

6.1.2. General Start Up Experiments.....	57
7. Results and Discussion .....	60
7.1 Raw data Evaluation – Residual Moisture .....	61
7.2. Statistical Evaluation - DoE.....	66
8. Washing and Purification Studies .....	72
9. Outlook and Conclusion.....	78
10. List of Literature.....	80

## ***Introduction***

As the ever increasing demand of product quality is required, innovative separation technologies have now an increasing role in pharmaceutical and chemical industries. [1]

Particularly when handling with slurries some form of solid-liquid separation is always used with the aim of:

- recovering and dewatering the desired solids (this may be followed by washing)
- recovering and cleaning the liquid
- separating the two phases from each other before recycling/ reusing both
- separating the two phases for environmental reasons. [2]

Because of this huge demand and the broad offer of filtration systems this Master Thesis has been written. A dynamic shear enhanced filtration system (DYNOTEST by Bokela) has been tested for recovering and dewatering a lactose suspension.

Attention has mainly been paid to the influences of the process parameters during dewatering the lactose suspension. In fact, cross-flow filtration is a pressure driven process, in which the pressure difference between inlet and outlet is known as the driving force of the process. This pressure difference, within the meaning of the occurrence of flow resistance, is affected by several factors. These factors were considered within a set of experiments and evaluated according to their influence on the residual moisture.

To do so a set of experiments were prepared in order to check the influences of the parameters, such as feed-rate, feed-concentration and the velocities occurring in front of the membrane. The evaluation was done by a statistical tool (Modde by Umetrics; Version 9.1), with the aim to predict the future robustness or capability of the investigated system.

# 1. Filtration

The principal of filtration is the separation of components from a fluid stream. In that case, the primary role of the membrane is a selective barrier, which can permit the passage of one component and retain others. By this definition the membrane is not defined as a solid, in this broadest sense a membrane could also be liquid or gaseous or a combination of them. The picture below shows a classification of various separation processes referring to their particle size and their application. [3]

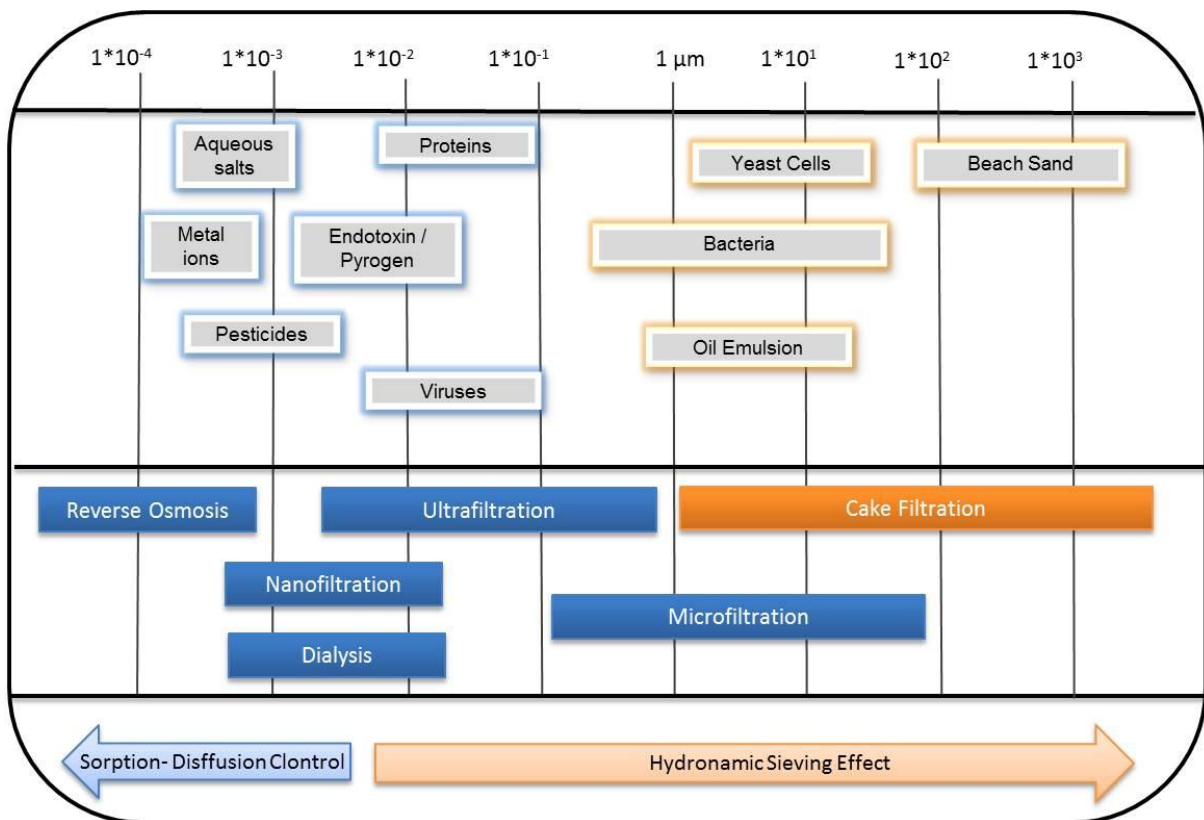


Figure 1: Filtration Spectrum [4]

## 1.1. Microfiltration

Microfiltration is a pressure- driven membrane process and based on physical separation, so that the pore size of the membrane is the crucial factor of retaining particles. As shown in Figure 1 microfiltration is placed between ultrafiltration and

coarse filtration (cake filtration) and operates in a range of particle size between  $0.1\ \mu\text{m}$  up to  $100\ \mu\text{m}$ . In this range of particle size, above  $10\ \mu\text{m}$ , the common separation techniques are often the coarse filtration which is conventional cake filtration methods. [3, 5]

The separation of particles in microfiltration is based on the sieve effect, so that one limitation to the separation is given by the outer surface of the membrane. The microporous structure of the membrane should have a narrow pore size distribution, in order to ensue quantitative retention of the particles for a given type and size. [6]

Common available membranes have a pore size between  $0.05\ \mu\text{m}$  up to  $10\ \mu\text{m}$ . Due to the pore size distribution, which is in most cases a broad distribution, the characteristic of membranes is its nominal pore diameter. Figure 2 shows a Polyvinylidenefluorid (PVDF) membrane with a nominal pore diameter of  $0.2\ \mu\text{m}$  which was used during the experiments. [6]



**Figure 2: Symmetric polyvinylidenefluoride membrane**

According to the above mentioned requirements, membranes used in microfiltration may be constructed from a wide variety of materials, including cellulose acetate (CA), polyvinylidenefluoride (PVDF), polyacrylonitrile (PAN), polypropylene (PP), polysulfone (PS), polyethersulfone (PES), or other polymers. [6]

Membranes based on inorganic materials are as well available. These are often ceramics or fiber-reinforced carbons. Inorganic materials are specifically marked by their extremely good thermal, chemical and mechanical resiliencies and are used when specific properties of the membrane are required. [6]



Materials, inter alia, differ in their wettability, whether the material is hydrophilic or not. For membranes based on polymers, it is necessary to prevent them from desiccation which could result in a change in physical and chemical properties. Since the membrane should be totally wetted during operation, hydrophobic membranes tend more often to foul by separation of aqueous dispersions. On the other hand hydrophobic membranes have its benefits in chemical and thermal resistances. Hydrophobic membranes are for instance polypropylene (PP) or polyvinylidenfluride (PVDF). For aqueous dispersion the wettability of hydrophobic material is poor, but if they once have been wetted aqueous solutions will all pass through. [3, 7]

In most cases the choice of the right membrane depends on the mode of operation affecting the life span of the membrane. The physical and chemical properties of the materials are often a crucial factor for the selection of a membrane. The material properties significantly impact the mechanical resistance of a membrane resulting in their operational life span. [3, 6]

Materials used as filters should ideally possess the following properties:

- chemical resistance
- mechanical stability
- thermal stability
- high permeability
- high selectivity
- stable operation

## 1.2. Techniques in Microfiltration

The main challenge in membrane filtration, is to ensure high permeate flow-rates. Retained particles build up a filter cake, as a direct consequence permeate flow-rate will decrease. [3, 6]

Therefore two differential techniques were established. They differ in their kind of operation, if it is a static (Dead- End- Filtration) or a dynamic (Cross- Flow- Filtration) operation. [6]

To choose the right technique, the characteristics of the fluid should be taken into consideration. Higher feed concentration leads to an increase in cake formation, consequently the application of a huge pressure drop must be given. [3, 6]

There are many applications where the suspension to be filtrated is highly concentrated. Particles or macromolecules such as cells, proteins and precipitates will rapidly compact on the filter surface. Consequently, the filtration rate drops quickly to an unacceptable level, when conventional cake filtration is the chosen technique. In these instances, a crossflow membrane system provides the means to maintain stable filtration rates. Dead-End techniques are useful when the concentration of particles to be removed is lower or the packing tendency of the filtered material does not produce a large pressure drop across the filter medium, as mentioned below. The demand of energy is given by the incessant increase of pressure and leads to an increase in costs. [8]

Whereas classical crossflow filtration systems are obtaining shear rates by increasing flow velocities, which is done by reducing tube diameter or channel thickness, dynamic shear enhanced techniques were established to control pressure independently from the flow velocities. While conventional crossflow systems generate large axial pressure gradients due to the typical tube construction, shear enhanced systems generate high shear rates by moving parts, such as a disk rotating near by a fixed membrane or by vibrating/rotating the membrane. Further information about shear- enhanced techniques are presented in chapter 1.1.3..

Shear enhanced techniques are very common, and permit to reach very high shear rates, of the order of  $(1-3) \times 10^5 \text{ s}^{-1}$  and to increase permeate flow rate. [9]

Eventhough these techniques are very common, the demand of energy should be taken into consideration. To avoid deposition of solid on the membrane turbulent flow characteristics are created. Often this is done by rotating components, which increase the cost of equipment. [3]

### 1.2.1. Dead- End- Filtration

Many simple filtration processes use a Dead-End technique, where the flow of the suspension to be filtered is directed perpendicular to the filter surface, as shown in Figure 1. According to the growth of the filter cake, flow resistance will increase leading to a decrease in permeate flow rate, shown in Figure 3. [10]

To obtain the fluid flow, a pressure drop has to be applied across the membrane. [10]

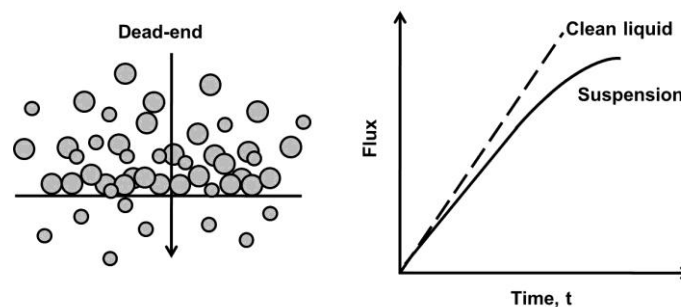


Figure 3: Princip of the Dead- End Filtration [10, 11]

The correlation between flow resistance and the applied pressure drop is given by Darcy's law. Relating to the flow rate the equation is given by:

$$J = \frac{A * \Delta p}{R * \mu}$$

Equation 1: Darcy's Law

Where:  $J$  = permeate flow-rate  
 $A$  = face area  
 $\Delta p$  = applied pressure  
 $R$  = total resistance      where  $R = R_m + R_c$   
 $\mu$  = dynamic viscosity

The total resistance, acting towards the pressure difference, is given by the membrane resistance ( $R_m$ ) and the resistance occurring due to the build up of a filter cake. In general, membrane resistance is the ability of a porous material to allow fluids to pass through it and can be evaluated by measuring the permeate flow-rate of pure water through a clean membrane. If the suspension is a clear liquid, all parameters in Equation 1 will be constant. A linear rise of the permeate flow-rate will be determined, shown in Figure 3. [10]

In practice, the suspension often includes particles, which deposit on the filter medium. The typical decrease in permeate flow-rate is the consequence out of the formation of a filter cake. Therefore to apply a constant permeate flow-rate, it is necessary to increase the pressure drop. Darcy's Law gives the relation between the applied pressure and permeate flow-rate. As shown in Equation 1 the pressure drop is direct proportional to the permeate flow-rate. [10]

The cake resistance in cake filtration systems is dominant, as it correlates with the pressure, and determines the filterability or how quickly a filtration could be performed. For prediction of the permeate flow-rate it is necessary to consider this effect so that the equation of Darcy should be written as follows

$$J = \frac{A * \Delta p}{\mu (R_m + R_c)}$$

**Equation 2**

$\alpha$  in this equation denotes the specific cake resistance. The total resistance resulting out of the filter cake is assumed to be proportional to the amount of cake deposition. So that cake resistance is given by

$$R_c = \alpha * m$$

**Equation 3**

where  $m$  is the cake mass per unit membrane area. For further treatments it is much easier to depict the cake mass as volume of filtrate  $[V]$  filtered in time. So that cake mass should be expressed as

$$m = \frac{cV}{A}$$

**Equation 4**

where  $c$  is the concentration of the solid in the suspension and  $A$  is again the membrane area. [10]

One of the classic methods to determine the specific cake resistance is to express flux as volume of filtrate as a function of time at constant pressure. So that flux could be rewritten in his reciprocal form, by consulting Equation 2 and Equation 4 as

$$\frac{t}{V} = \alpha\mu c \frac{V}{A^2 \Delta p} + \frac{\mu R}{A \Delta p}$$

**Equation 5**

By plotting  $t/V$  against the measured volume of the filtrate, the slope will determine the specific cake resistance as

$$\frac{\alpha\mu c}{2A^2 \Delta p}$$

**Equation 6**

Out of this relation, the specific cake resistance could be easily calculated, since the pressure is constant and the membrane area should be known as well. The fluid viscosity needs to be determined first. [10]

Another option to determine the specific cake resistance is the use of the Equation of Kozeny and Carmen proposed that the pore space of a porous bed of a powder has the same characteristic as the pore space of a bundle of parallel capillary tubes. Based on Hagen Poiseuille's Law for a fluid flow through capillary tubes, the Carmen-Kozeny Equation is given by

---

$$\alpha = \frac{KS_V^2}{\rho_c} \frac{1 - \varepsilon}{\varepsilon^3}$$

Equation 7

Where:  $\alpha$  = specific cake resistance  
K = Kozeny constant; depends on particle size, shape and porosity  
 $S_V^2$  = mean particle surface area per unit volume  
 $\rho_c$  = density of the solid  
 $\varepsilon$  = cake porosity

The importance of Equation 6 in filtration processes is limited, too many unknown factors needed to be determined first, such as cake porosity and the Kozeny constant. [10]

However, in practice, due to an increase of resistance, this build up of a filter cake is generally unwanted. Several methods are available which should prevent the build up of a filter cake. Periodic back washing is one method to apply higher permeate flow-rate and is commonly used in Dead-End operation mode. [6]

During processing, the decrease in flux flow rate is compensated by an increase in feed pressure. The variation of the applied pressure reaches from about 0.5 till 2.5 bar. After exceeding the maximum feedpressure, a removal of the filter cake is necessary to apply acceptable flow rates. In practice, this is done by changing the flow direction through the membrane, by increasing pressure on the site of the filtrate. Consequently the backflush removes or carries off the filter cake. Repeated backwashing units are required to achieve maximal permeate flow within one filtration step. Nevertheless backwashing causes delays in processing time, and can only be performed batchwise. [6]

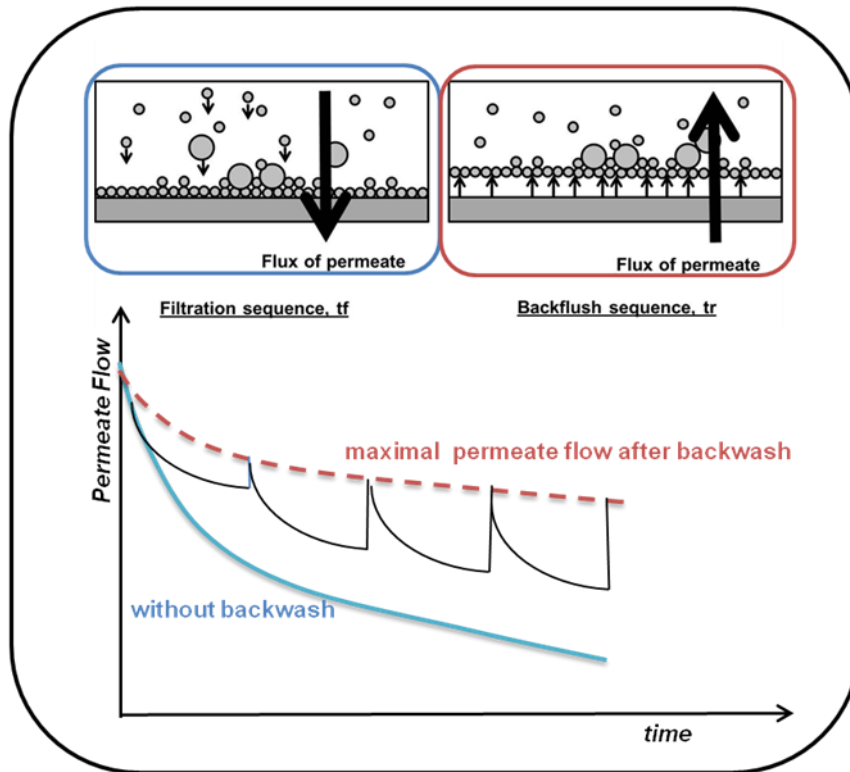


Figure 4: Methods for Backflush [12]

### 1.2.2. Cross- Flow- Filtration

As shown in Figure 5, in cross- flow- filtration mode, the suspension to be filtrated, flows parallel to the membrane. In that case, the formation of filter cake is reduced, and a better filtration rate is given over time. [13]

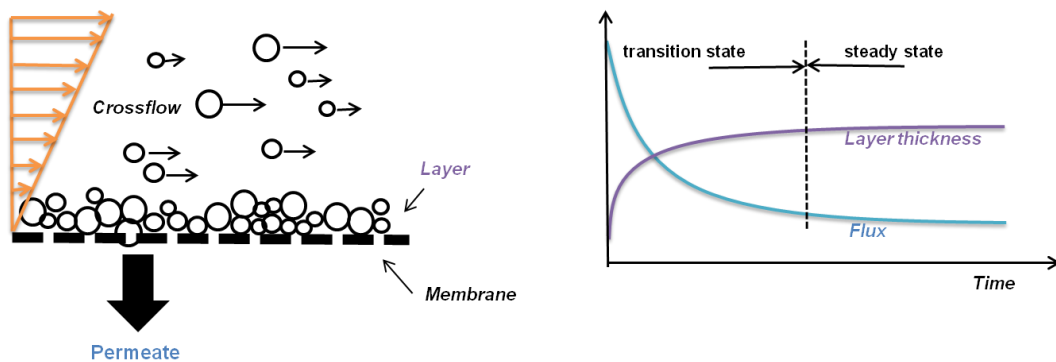


Figure 5: Principe of Cross- Flow Filtration [13]

There are various parameters directly effecting the permeate flow-rate. Such as cross flow velocity, transmembrane pressure, membrane resistance, layer resistance, size distribution of the suspended particles, particle form, agglomeration behaviour and surface effects of the particles etc., should be taken into consideration. [13]

The generation of a cross flow along the membrane is only one opportunity to reduce the build up of a filter cake. In industrial applications, this is done by channel or tube constructions, increasing flow velocities and therefore wall shear- stress by reducing tube diameters. As a consequence the build up of the filter cake is kept on a minimum and a quasi- steady permeate flow-rate could be generated. [6]

Figure 5 shows the characteristic curve of a permeate flow-rate. During the run-in period, the filter cake grows and leads to the typical decrease in permeate flow-rate by an increased flow resistance. The steady state is reached when a constant filter cake deposition is observed. [13]

To sume up, there are two possibilitys, which effect the wall shear stress

- An increase in flow velocity
- Or a reduction of the hydraulic diameter

There are several types of industrial dynamic filtration systems available, all based on the principle of enhancing wall shear stress [6, 9, 3]

The main challenge was to decouple the increasing pressure from flow velocities by increasing simultaneously wall shear stress. In newer systems this is done by rotating parts within the filtration system.

### **1.2.3. Dynamic shear-enhanced membrane filtration**

The following section contains the realization and the possible practical implementation of generating high shear rates. [9]

In modern constructions of dynamic filtration, higher shear rates are realized by moving parts, such as rotating membranes, or vibrating membranes and disks



rotating near by a fixed membrane. This is based on an increase in tangential fluid velocity, which as already mentioned leads to less particle deposition. [9]

Drawbacks are the complexity and limitations in membrane area, which cause a raise in equipment costs. The consensus of all techniques is a moving part of the equipment. This causes a higher energy demand and also leads to an raise of costs. The next three subitems discuss commercial available dynamic filtration systems. [9]

### 1.2.3.1. Rotating Cylindrical Membranes

Rotating cylindrical membrane systems were first commercialized in the mid-1980s, and were based on a couette flow typ. Figure 6 shows a typical construction, adapted from its application in medical processes. In that case it is used to separate placsm cells from blood. It is built up from a stationary outer cylinder and another rotating one in the middle of the equipment, while this inner one consists of the membrane.

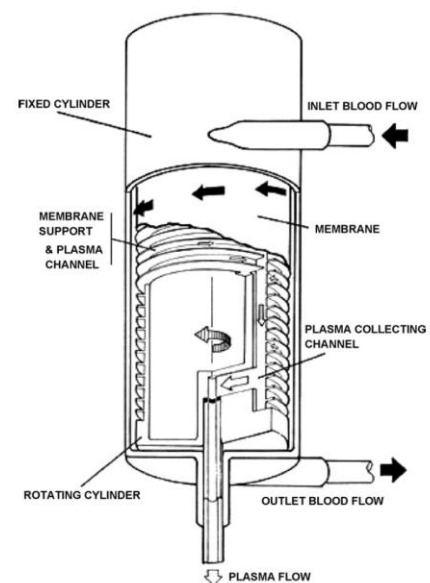


Figure 6: Rotating Cylindrical Membrane [9]

The suspension is pumped through the axial gap of these two cylinders, when a certain speed of rotation is reached, counter rotating vortices, so called Taylor-vortices, are induced. This causes a transport away from the membrane surface, and leads to an increase in shear rate, which are ten times higher than in conventional available cross flow systems. Depending on the high shear rate permeate flow-rate will also reach three to 20 times higher throughputs. [3, 9]

### 1.2.3.2. Vibrating Systems

Vibrating systems, such as the Vibrating Shear Enhanced Processing (VSEP) was invented by Dr. J. Brad Culkin in 1985, and is today produced by New Logic Research, Inc.. Instead of rotating components the enhancement of the shear rate is realized by vibrating the membrane. It consists of a stack of membranes separated from each other by gaskets and permeate collectors, which is shown in Figure 7. This stack is placed on a vibrating base, which translates the torsion force into an oscillation, this motion can reach shear rates up to  $150\,000\text{ s}^{-1}$ , which are ten times higher than a commercial available cross flow systems. The torsion spring is shown in the Figure 7. [9]

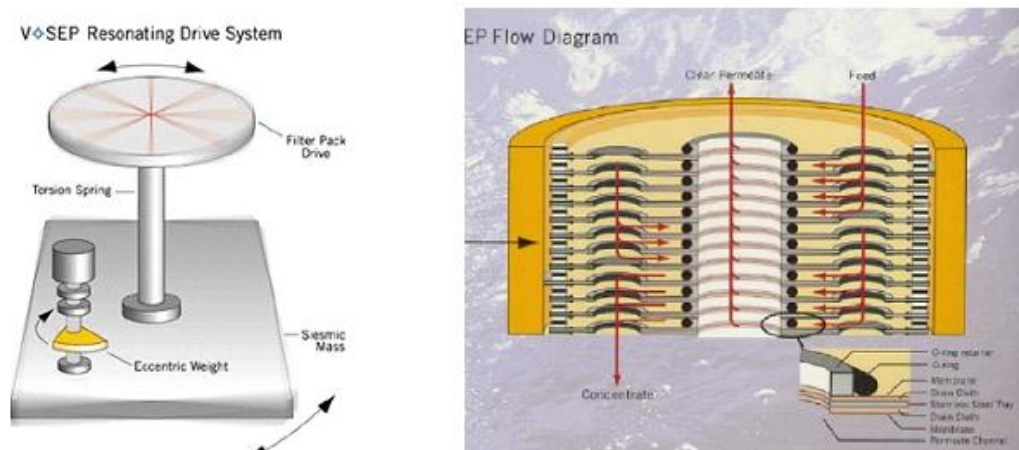


Figure 7: Vibratory Shear Enhanced Process [9, 25]

### 1.2.3.3. Rotating Disk Systems

The dynamic membrane filtration with a rotating disk system is a very versatile cross flow process for micro-, ultra- or diafiltration of micro- to nano-sized particles in slurry. Applications like

- separation of solids
- concentration or
- washing

of highly concentrated slurries are performed in a continuous operation or in batch mode. [14]

Bokela for instance developed a multi disk system, the so called Dyno Filter, which is shown in Figure 8.

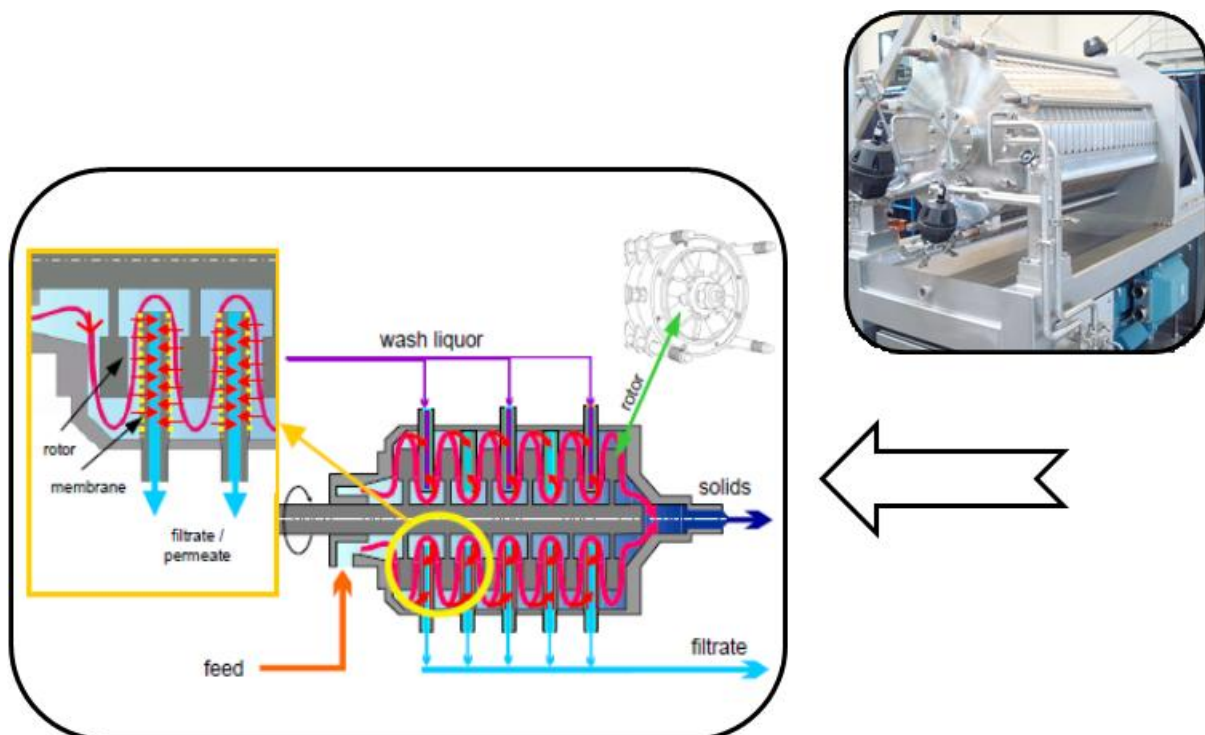


Figure 8: Schematic plant- layout of the Bokela system [14]

Based on the principle of the dynamic cross flow filtration, the Dyno Filter consists of several filter modules, which are arranged in series. Each chamber includes the membrane. [14]

Rotors in front of the membrane generating the tangential cross flow and ensure furthermore a homogenous mixing of the slurry. Another benefit is given by the high velocity gradient and induced high shear rates over the filter medium, which avoid the blocking of the filter. [14, 9]

The slurry flows meander-like through the chambers and becomes more and more concentrated. The retentate is extracted with an automatic drain valve. This valve could be controlled by the power demand of the rotor. While the viscosity increases, the assumed power demand of the rotor shaft increases too. In a further consequence the discharge of the retentate could be controlled by the rise in bulk concentration. Figure 8 shows the full-scale plant for pharmaceutical applications. [14]

According to the serial arrangement of the filtration chambers and the homogeneous mixing of the slurry, due to the turbulence, washing and extraction is more effective. Furthermore the input of wash water or any other wash liquid can be varied on demand. [14]

Some Apparatus Data are given below:

- Filtration area: 0.013 m<sup>2</sup> - 8 m<sup>2</sup>
- Number of modules: 1 - 20
- Diameter of the modules: 145 - 550 mm
- Hermetically sealed, explosion-proof system
- Automated and self-cleaning process
- Maximum filtration pressure: 6 bar, abs.
- Maximum process temperature: 100 °C (up to 200°C for specific applications)
- Low to moderate rotor speeds (depending on the filter size), i.e. no contamination by abrasion

The separation of solid content in the range of nanometer up to micrometer is feasible. Due to the set-up high throughputs even for highly concentrated suspensions with high viscosity are given.

The integrated cooling system allows cooling or warming up the filtration chamber. This is convenient if the suspension to be filtered produces a lot of internally friction heat. Whereas conventional cross flow filters (e.g. with tubes) achieve final concentrations of 10-20 Vol-%, Bokela predicts that the DYNO Filter produces final concentrations up to 65 Vol-% in one step. This assumption is shown in Figure 9. [14]

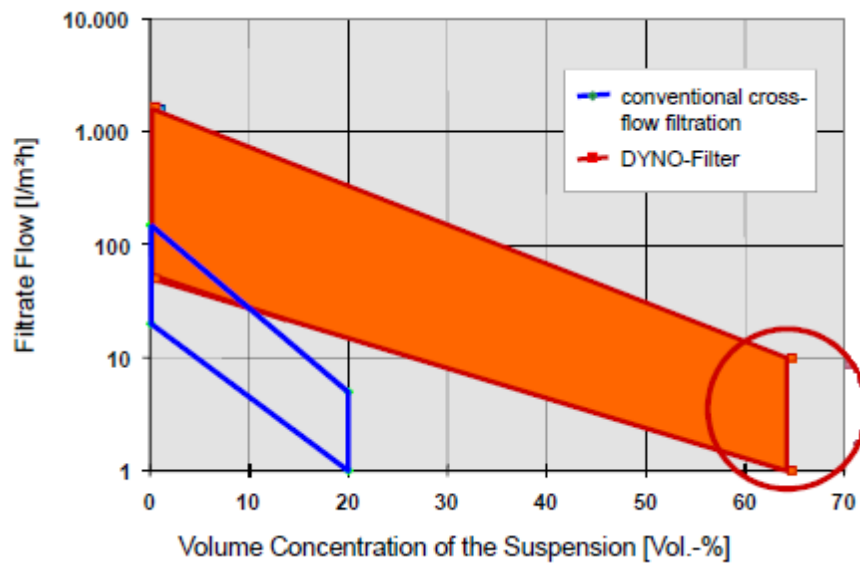


Figure 9: Comparisson of conventional Cross Flow Filtration and the DYNO Filter [14]

Bokela also offers the possibility of a filtration unit for a Lab plant. The DynoTest is a laboratory apparatus for the simulation of the cross-flow filtration. The filter consists of one chamber and can be operated batch-wise or continuously, depending on its configuration. All data such as pressure, rotor speed, range of concentration and flow rate are collected by the software and enable to analyze the thickening, the washing and classification out of the filter cake. [14]

## 2. Theoretical Background

For industrial applications the knowhow of prediction of flow rate and the corresponding separation efficiency is important. Though there are several theoretical and empirical methods available, none of them are totally satisfying. The theoretical approaches are mainly based on the mass transfer, which should lead to a better understanding of the predominant phenomena along the membrane. Several adoptions of the mass transfer model are available, including different hydrodynamic and thermodynamic boundary conditions as well as physical- chemical properties of the particles. Consequently, due to considering all of these phenomena, these models are often too complex for a simple use. [6]

Models for the description of the membrane processes can be distinguished into empirical and theoretical models. While the empirical models are useful in practice, for predictions of flow rates, theoretical models are useful for the basic understanding of the processes during cross-flow filtration. [13]

Filtration performance models are generally expressed in terms of flux flow rate  $J$ , which is the volume of suspension that passes through unit membrane area in unit time. [3, 6]

There are many factors affecting this flux flow rate. The build-up of a filter cake, causes an initially decrease in permeate flux. Phenomena, such as concentration polarization, membrane fouling and at least membrane blocking leads to a steep decline in flux flow rate. [6]

One model for expressing flux flow rate is the so called "film model" or "mass transfer model". This mathematical model is based on diffusion. The diffusive movement causes a particle transport in contrast to the convective transport. [3, 13]

## 2.1. Mass Transfer Model and Concentration Polarization

The convective transport of the fluid could be expressed by

$$J_S = J * C_B$$

Equation 8

Inhere  $C_B$  is the bulk concentration. [3]

Along the membrane, a concentration gradient occurs, resulting from the convective transport of the particles and their deposition on the mebrane. The difference in local concentrations causes a back transport of solid into the bulk based on diffusion. This effect known as concentration polarization is shown in Figure 10. [3]

The back transport of the particles could be expressed as followes

$$J_S = D * \frac{dc}{dx}$$

Equation 9

The driving force of the solid back transport is independent of pressure and only affected by the concentration gradient  $[\frac{dc}{dx}]$ . The proportionality factor  $D$  represents the diffusion coefficient. [3]

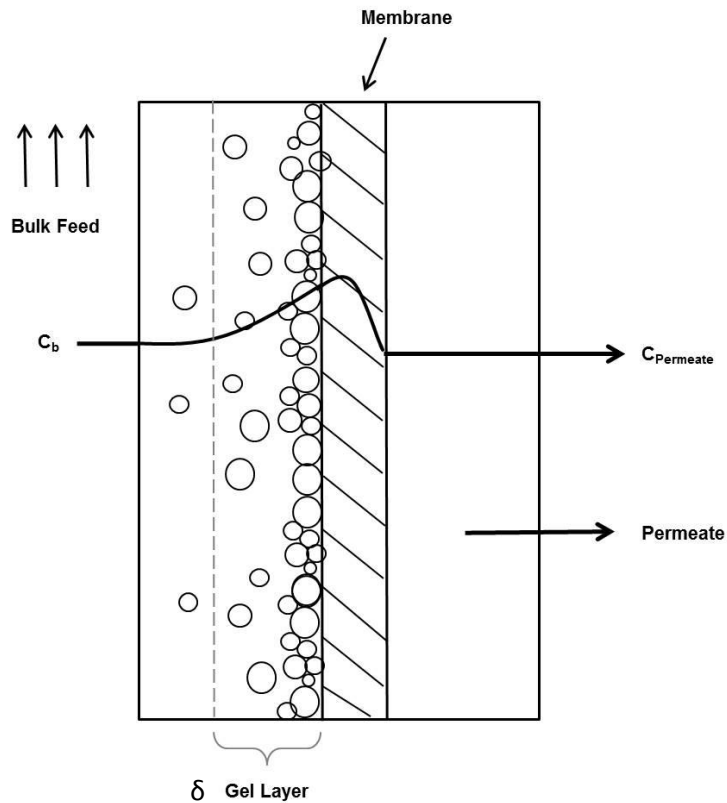


Figure 10: Concentration gradient along the membrane and back diffusion [15]

At equilibrium, so-called the steady state, both transport mechanisms, will balance each other. [3]

Under these conditions, the permeate flow-rate could be calculated as follows:

$$J = \frac{D}{\delta} * \ln \frac{C_G}{C_B} = k * \ln \frac{C_G}{C_B}$$

Equation 10

$C_G$  is the solid concentration on the membrane, also called “gel” concentration.

As shown in Figure 10,  $\delta$  is the thickness of the boundary layer through which the concentration gradient exists. The ratio between diffusion coefficient and thickness of the layer, expressed as  $k$ , determines the mass transfer coefficient.

Mentionable is that there is no pressure dependent term in this equation. Consequently permeate flow-rate is only limited by the rate of back- transport of solid



into the bulk. Furthermore permeate flow-rate can only be obtained by enhancing  $k$ , which is done by reducing the thickness of the boundary layer. Figure 11 shows the typical turbulent boundary layer profile.

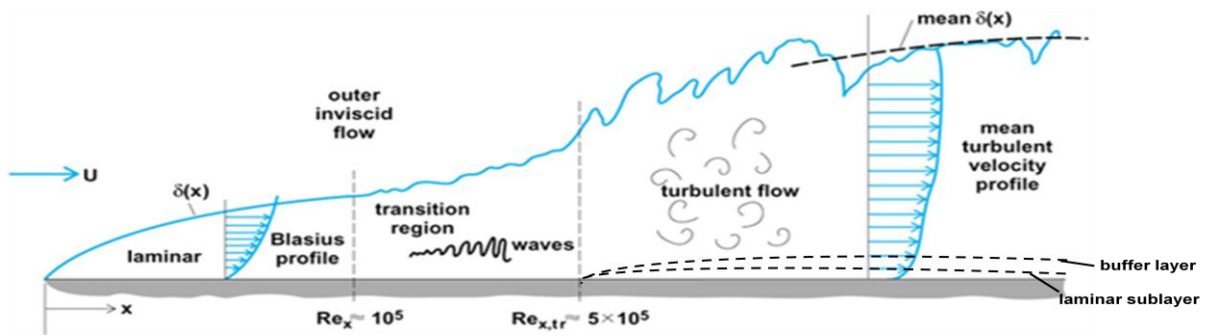


Figure 11: Schematic description of a turbulent boundary layer [16]

The flow characteristic changes into fully turbulent by exceeding the critical Reynolds' number ( $Re_{tr} \sim 5 \cdot 10^5$ ). Time-dependent variations of the flow characteristic is the consequence. In addition to the turbulent regions, a laminar sublayer is formed at the membrane, where the velocity of the fluid becomes zero. Accordingly, the formation of a thin particle-deposition layer cannot be fully avoided.

According to Equation 10, the concentration of the gel layer and the mass transfer coefficient can be calculated by plotting the permeate flow-rate against their bulk concentration ( $x$ - axis, logarithmic). The slope and the intercept determine the mass transfer coefficient and the gel layer concentration, shown in Figure 12. [5]

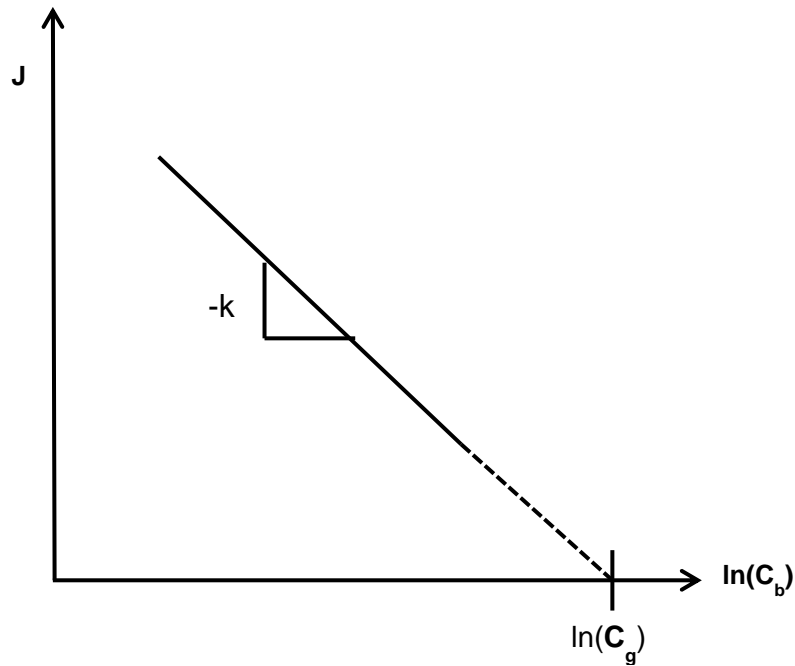


Figure 12: Determining the mass transfer coefficient

Consequently the Mass Transfer Model is based on the following facts [5]:

- The filtration rate is independent of the transmembrane pressure.
- The filtration rate is decreasing directly proportional to the logarithm of the concentration of the retained particles.
- The maximum concentration possible to reach is the gel concentration.
- The mass transfer coefficient is depending on flow conditions.

In practice the reduction of the layer height is often done by changing the flow conditions in the filter chamber, as already shown during introduction of shear enhanced filtration systems. The easiest way to get an increase of turbulences is of course an increase of feed flow rate, either this is done by moving parts inside the filtration chamber or by increasing the pressure difference. This increase of flow velocities leads to an decrease of the layer thickness and influences therefore directly the mass transfer coefficient. As a consequence the boundary layer height as well as the amount of back-diffusion remains small due to the lowered deposition layer (laminar sublayer). Thus the turbulent boundary layer and accordingly the laminar

sublayer are tried to kept rather low, membrane fouling and adsorption is one of the most crucial factor of decreasing permeate flow-rate. [3]

### **2.1.1. Membrane fouling**

Within the topic above, the deposition of solids, and the occurrence of a concentration gradient was discussed. This section concerns the formation of a fouling layer, which is not to be confused with the above described polarization layer also called gel layer. Fouling appears from solute-membrane interaction. Every solute within the feed stream and every solid compound can interact in a different way with the membrane, a general rule for membrane fouling does therefore not exist. Interactions are given due to conformation charge, zeta potential, hydrophobicity and other properties which can significant affect membrane fouling. Attention should also be paid to predominant operating parameters which also affect or assist membrane fouling. [3, 6]

In general fouling is a loss of performance due to contamination. Fouling is classified into reversible fouling, that could be easily reversed by washing, and irreversible fouling. Concentration polarization or gel layer formation is understood as a mechanism of reversible fouling. The mechanism of concentration polarization is explained in Chapter 2.1.. Adsorption of macromolecules as well as formation of a filter cake, which blocks the pores, are the expected mechanisms of irreversible fouling. [17]

As a consequence permeability of the membrane decreases while flow resistance is increasing. The build up of this covering layer causes a change in membrane characteristics due to chemical and physical properties of the bulk.

The consequence out of this several mechanisms of membrane fouling is a increase of pressure, due to simultaneously increase of the flow resistance. Meanwhile permeate flow-rate will decrease. Figure 13 shows schematically membrane fouling. [6, 17]

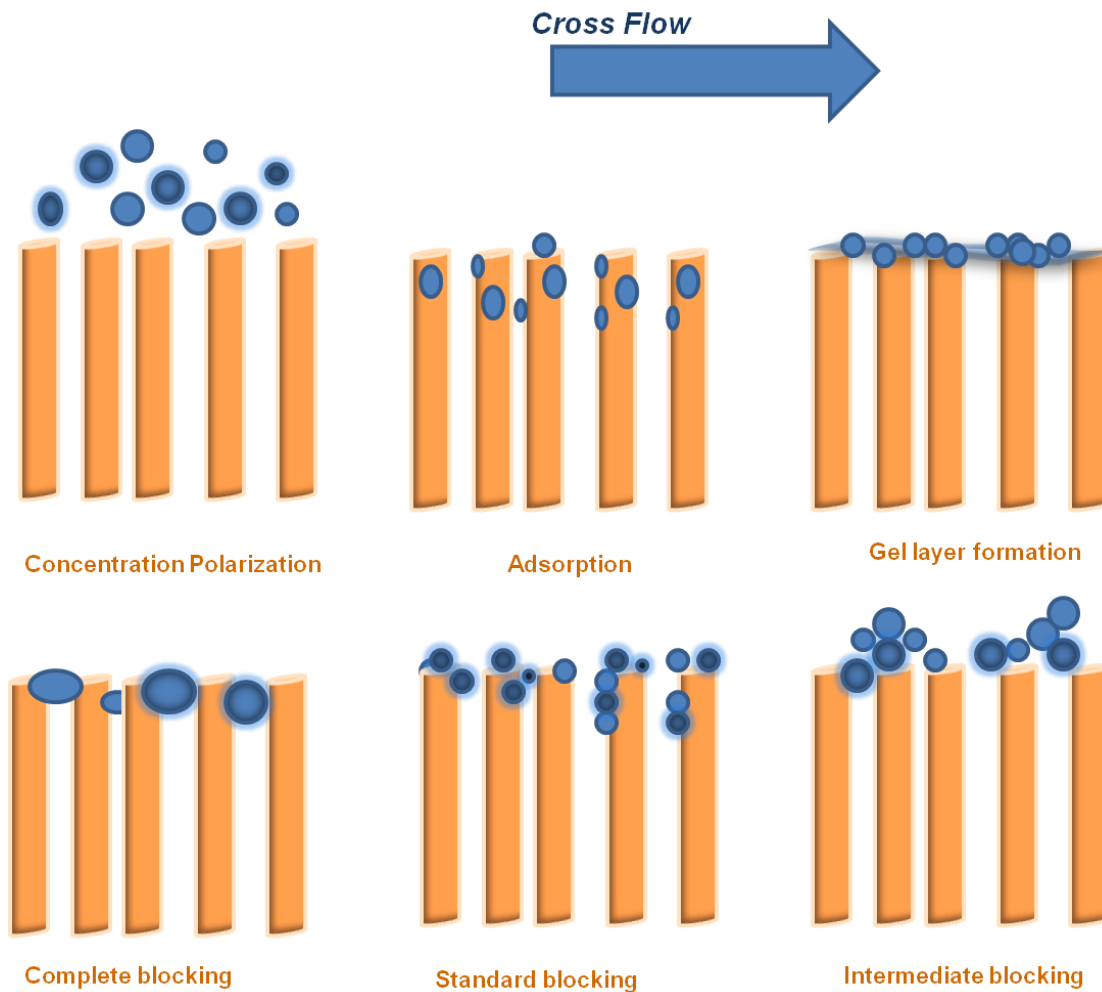


Figure 13: Types of pore blocking [17]

Operating parameters, such as pressure conditions and flow rates, influences as well particle deposition on the membrane. [3, 6] High shear should hinder the effect of particle deposition. However, at higher feed-rates larger particles will be affected by an increased lateral lift force resulting in a movement off the membrane. Due to the different impact of lift force on the particles a consequence will be a stratification of smaller particles which will foul the membrane to greater extent. The effect of lift force is shown in Figure 14. [3]

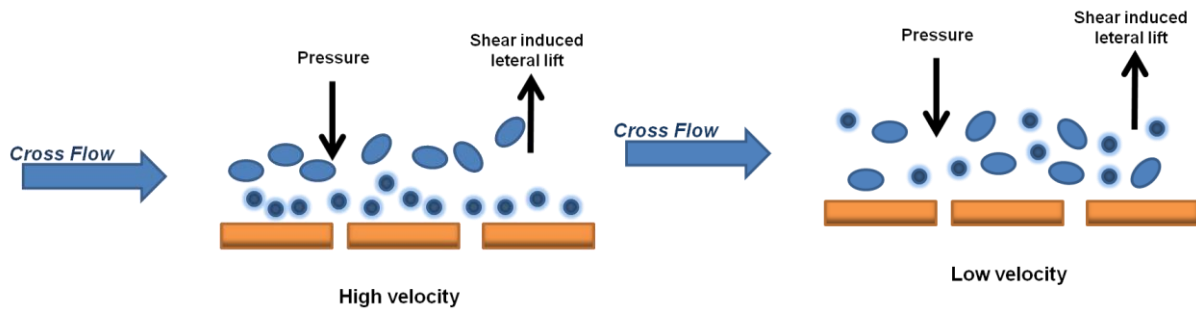


Figure 14: Fouling by particles of mixed sizes [3]

High pressure conditions show as well similar effects on fouling layers. Under the impact of high pressure, particles move to the membrane much faster than they could be removed by shear. [3]

To summarize, membrane fouling and / or blocking cause a deep loss in performance. The permeability of the membrane decreases due to the deposition which reduces at least membrane surface, as a consequence permeate flow decreases. [3, 6, 17]

## 2.2. Permeate flow-rate declaim

The filtration system throughput or the productivity is characterized by expressions of permeate flow-rate. Permeate flow-rate, at its simplest form, can be expressed as follows

$$\text{Permeate flow - rate} = \frac{\text{Driving Force}}{\text{Resistance}}$$

Equation 11

The resistance in series model is the most generally applicable one, and based on the assumption that there are several factors effecting the flow resistance. [18]

The driving force of a fluid through a porous medium in micro- ultra- filtration applications, is the pressure gradient occurring along the membrane. This pressure

gradient is so-called the transmembrane pressure (TMP). The TMP is defined as the pressure difference between the inlet pressure, or feed pressure, and the filtrate pressure. [19]

$$TMP = \frac{p_f - p_c}{2} - p_p$$

Equation 12

Where  $p_f$  is the feed pressure (inlet pressure),  $p_c$  is the concentrate pressure and  $p_p$  is the pressure on the permeate side (outlet pressure). [19]

The total resistance affecting the flow rate, acting in opposition to the driving force, is assumed to be the membrane resistance and the resistance according to the build up of a filter cake and can be written as follows

$$R_t = R_m + R_{ads} + R_{cp} + R_g$$

Equation 13

Where:

- $R_t$  = total membrane resistance
- $R_m$  = intrinsic membrane resistance
- $R_{ads}$  = resistance of solvent adsorbed onto the membrane surface
- $R_{cp}$  = resistance of the concentration boundary layer
- $R_g$  = resistance of concentrate at the membrane surface (gel layer)

While the intrinsic resistance of the membrane is assumed to be constant, and can also be obtained from the membrane manufacturer, the resistance occurring due to adsorption and the filter cake fluctuates. The fluctuation of values in cake resistances are resulting out of the permanent removal of the filter cake, which is especially observed in dynamic filtration systems.

Figure 15 shows the shear depending permeate flow-rate during dynamic filtration [19]

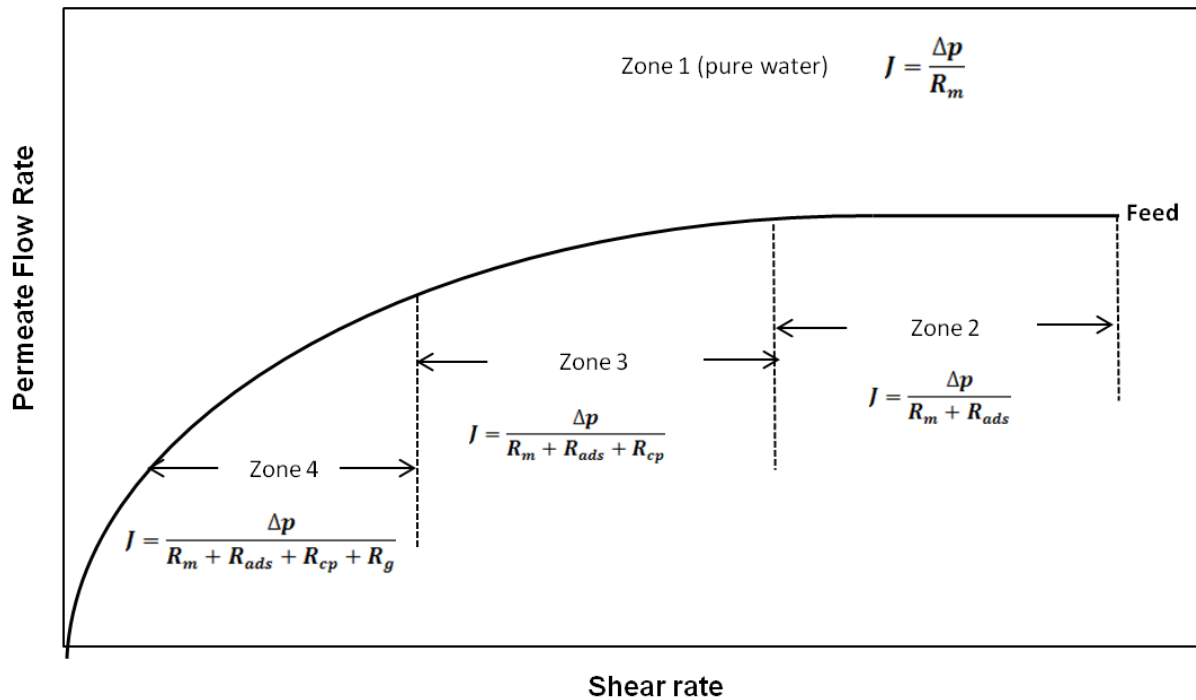


Figure 15: Resistance in series model [18]

Changes in shear rate directly influence the permeate flow-rate. If the shear rate decreases the permeate flow-rate will decrease as well which happens due to the preferred particle deposition. The shear rate therefore effects not only the thickness of the boundary layer, but also the kind of particle deposition. If the shear rate is high enough the resistance of adsorbed solute is obtained, and kept on a minimum (Zone 2). Theoretically the occurrence of a concentration gradient can be avoided, due to a hindered deposition of particles. Whereas if the shear rate decreases a concentration boundary layer will be established (Zone 3), which is shown in Figure 15. [18]

Jönsson et al. observed that, if the initial permeate flow-rate can be regained by increasing the shear rate, it is meant to be the build up of a concentration boundary layer. Finally, by further reducing the shear rate, Zone 4 will be reached where it is not possible to regain the initial permeate flow-rate. Flow resistance is than given by the build up of a filter cake (or gel layer), which is irreversible, even if the shear rate is again increasing. [18]

The resistance in series model can be a very useful tool during practical application. Accordingly, decreases in permeate flow-rate can be easily detected if it is a reversible phenomena or an irreversible one. Since the establishment of a concentration boundary is reversible a short interruption of the permeate flow should at least regain the initial permeate flow rate. Interrupting the permeate flow and applying a pressure on the permeate side is often done in microfiltration (back-flushing). [18]

The influence of shear rate on permeate flow-rate was already discussed in chapter 1. By enhancing the shear rate on the membrane, concentration polarization is kept on a minimum. Nevertheless the thickness of the boundary layer is mainly ruled by the operating pressure conditions, which influence the convective transport to the membrane. [18]



### 3. Quality by Design (QbD)

QbD, Quality by Design, is a scientific risk-based approach to pharmaceutical development. Both the industry and the FDA move toward establishing a concept in order to industry's understanding of the product and manufacturing process starting to assure high quality. [20]

The concept and definition of Quality by Design (QbD) are basically described in the guideline ICHQ8:

*A systematic approach to development that begins with predefined objectives and emphasizes product and process understanding and process control, based on sound science and quality risk management.* [21]

Therefore, when designing and developing a product, the first step is to define a product performance and identify the CQAs. [20]

The definition of a Critical Quality Attribute (CQA), is given by:

*A physical, chemical, biological or microbiological property or characteristic that should be within an appropriate limit, range, or distribution to ensure the desired product quality. (ICHQ8)* [21]

On the basis of this information, the industry is able to design the product formulation and process to combine those product attributes. According to this, a better understanding of the impact of the raw material attributes and process parameter on the CQAs is given, which leads to an identification and the control of sources of variability. [20]

As an outcome of all this basic knowledge, the industry can continually monitor and update its manufacturing process to assure consistent product quality. [20]

### 3.1. QbD Implementation

As already mentioned, to assure high quality the knowledge of the impact of the raw materials attributes as well as the knowledge of the impact of the process parameter must be well understood. Consequently the process needed to be continually monitored and updated to assure consistent quality over time. Figure 16 shows the different phases during the life cycle of a pharmaceutical process: define, design, characterize, validate, and monitor and control. [20, 22]

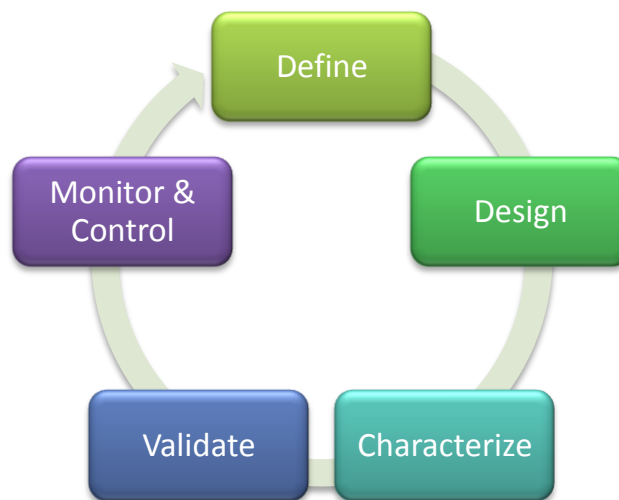


Figure 16: The life cycle of a pharmaceutical process [23]

The final link between "monitor and control" and "define" represents process changes during monitoring. Changes in process control monitoring would cause a definition, in that case, once again a definition of a design space is necessary. [23]

The International Conference on Harmonization (ICH) guidelines define a design space as:

*The multidimensional combination and interaction of input variables (e.g., material attributes) and process parameters that have been demonstrated to provide assurance of quality. Working within the design space is not considered as a change. Movement out of the design space is considered to be a change and would normally*

*initiate a regulatory post approval change process. Design space is proposed by the applicant and is subject to regulatory assessment and approval (ICH Q8). [21]*

The operating ranges in the manufacturing procedures are defined by a set up of experiments.

Figure 17 shows the key steps in process characterization. [20, 21, 23]

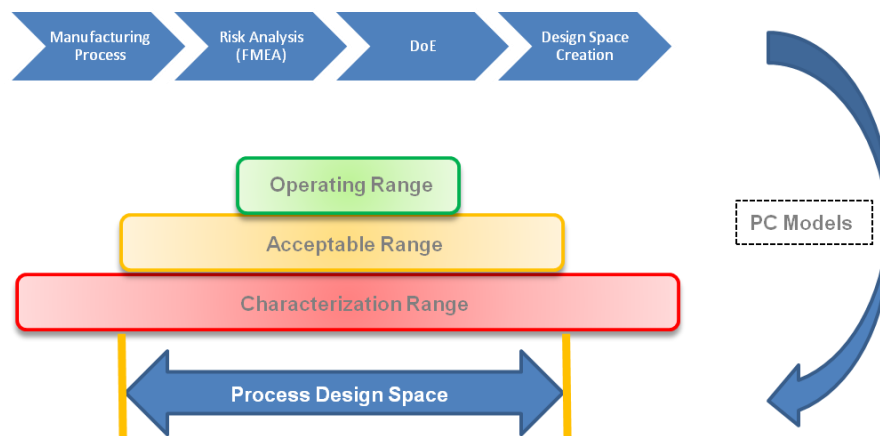


Figure 17: Key steps in process characterization [23]

First, a risk analysis is performed to identify parameters for process characterization. Second, studies are designed using design of experiments (DoE) so that the resulting data will be amenable for use in understanding and defining the design space. Third, the studies are executed and the results analyzed for decisions about the criticality of the parameters and about establishing the design space. [23]

### 3.2. Design of Experiment (DoE)

A DoE is used to gain a basic knowledge and increased understanding of new products and processes. The aim is to get a set of representative experiments, in which all factors, with direct influence on product quality, under investigation are varied simultaneously. [20]

The DoE is a statistical tool, that minimizes the number of experiments, to determine the relationship between impacts (inputs) and target variables (output), and consequently to generate as much information as possible. [20]

In common used experiments often only one separate factor at the time is changed, which does not lead to a real optimum. Factors are process-settings changed in the experiment. However by changing only one factor at the time the number of experiments increases which is time and cost intensive. Further these results ignore the quantitative interaction between these factors. [20]

In DoE the entire region in-between predefined interval is investigated in an organized way. Results of a DoE study allow the calculation of response surface (design space), which leads to the prediction of quality. Responses are predefined product parameters. In the case of this studies, responses are listed in Chapter 3.4.. [20, 23]

To define a suitable and statistically predictive model the definition of factors and responses need to be done first. A useful tool to define factors effecting process parameters is the fishbone diagram. For this study the software Modde V9.1 from Umetrics (Umetrics Inc./USA) was used to set up the experimental plan and to evaluate and interpret the experimental results. Figure 18 shows the key steps of generating a DoE and the use of it. [20]

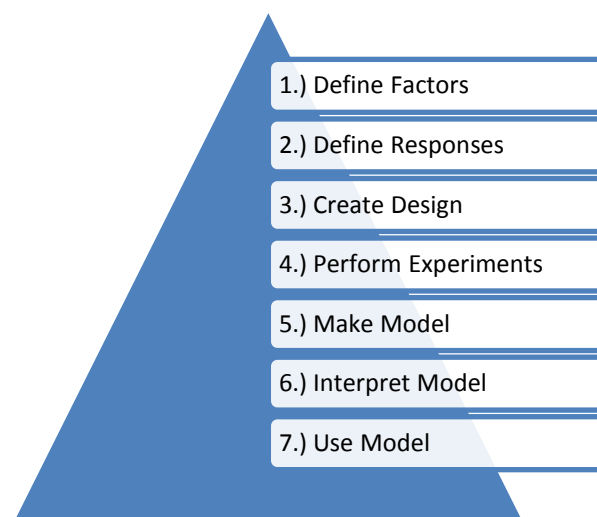


Figure 18: Key steps to generating a DoE

### 3.3. Analysis DynoTest Trials

Setting up the DoE for analysing the DynoTest a two-level full factorial design was chosen. [20]

A full factorial design is based on two values, a minimum and a maximum value. In-between a centre point, according to the arithmetic middle, is placed to guarantee reproducibility. This design consists of factors, each with discrete possible values or "levels", and whose experimental units take on all possible combinations of these levels across all such factors. Such an experiment allows studying the effect of each factor on the response variable, as well as the effects of interactions between factors on the response variable. [20]

For example, with two factors each taking two levels, a factorial experiment would have four treatment combinations in total, and is usually called a 2x2 factorial design. [20]

Figure 19 shows the concept of a DoE. Every experiment design has inputs and outputs. Inputs are factors effecting critical product qualities. Considerations out of a fishbone diagram lead to the predefined CQAs and as a result to the factors affecting the product quality. Whereas outputs or responses are the critical product qualities and needed to be measured and detected during the whole process. The responses, at least, should give information about optimal operation range. [20]

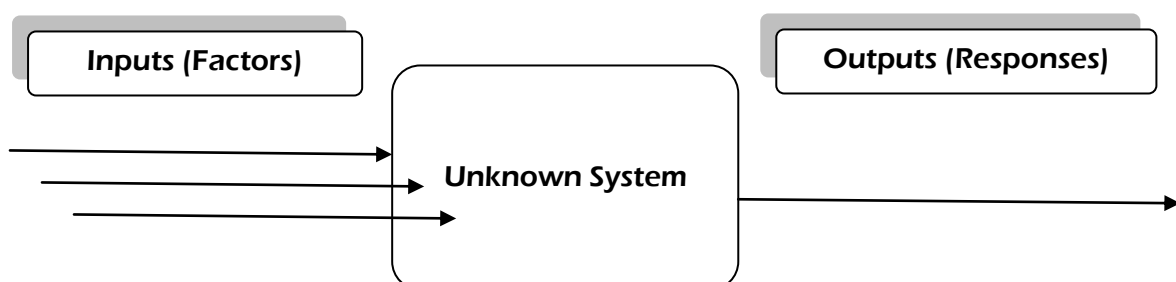


Figure 19: Concept of a DoE

### 3.4. Main DoE description

The aim of this working package is to investigate the operational behaviour of a small scale dynamic cross flow filter, in regard to the residual moisture. The impacts of different process parameters should be analyzed. As a first step a Fishbone Diagram according to all impacts was prepared, shown in Figure 20. Resulting coherences lead to the definition of factors and responses.

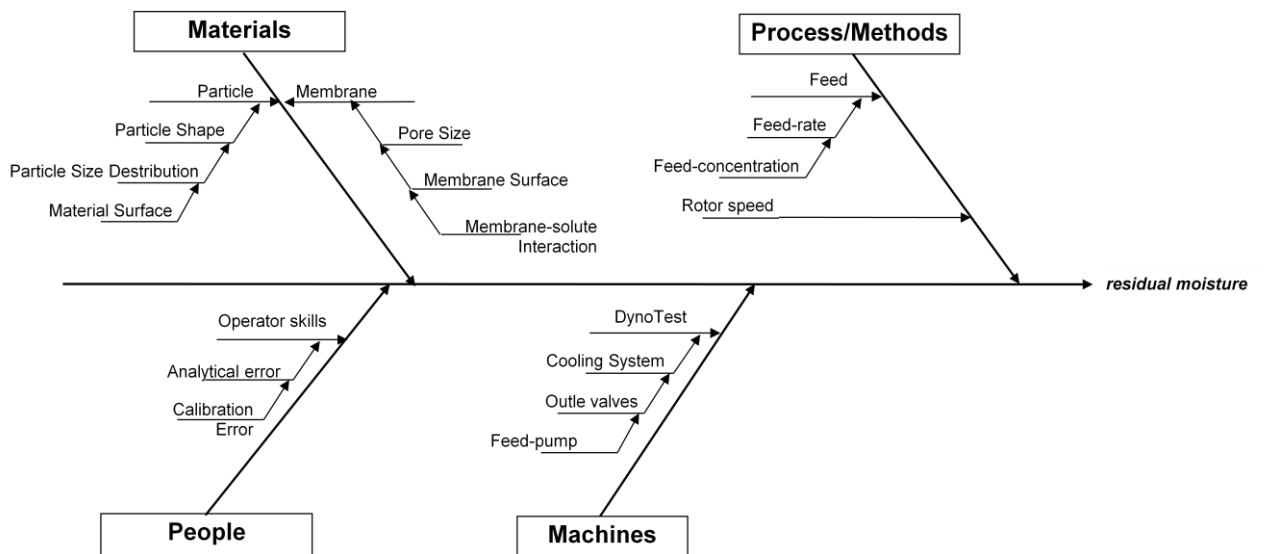


Figure 20: Fishbone Diagram

Table 1 shows the variable process parameters (factors) of the working packages resulting from first considerations.

<b>Factors</b>	<b>Type</b>	<b>Low</b>	<b>High</b>	<b>Center points</b>
<b>feed rate</b>	Controlled	13 L/h	61 L/h	37 L/h
<b>feed concentration</b>	Controlled	5 wt%	15 wt%	10 wt%
<b>outlet valve trigger</b>	Controlled	12 %	16 %	14 %
<b>rotor speed</b>	Controlled	800 rpm	1500 rpm	1150 rpm
<b>model substance</b>	constant (Granulac)			
<b>pore size of the membrane</b>	constant (0,05 $\mu\text{m}$ )			

**Table 1: Full factorial design for DoE1**

The variable process parameters were:

- 1) feed rate
- 2) feed concentration
- 3) outlet valve trigger
- 4) rotor speed.

To evaluate the effect of the DynoTest's process variables on the output parameter a set of design of experiments (DoE) was prepared. For each process variable a maximum and a minimum value were defined. Centre points were placed at the corresponding mean values. Centre point cases were repeated three times to check experimental reproducibility.

**Feed material:** DoE 1 was prepared with Lactose, due to its chemical and physical properties. Substance characteristics are listed in chapter 4.

**Feed rate:** The feed rate varied between 13 L/h and 61 L/h. While 61 L/h being the maximal limit of the feed pump, 13 L/h was chosen to be the lowest level just to prevent sedimentation of material within the supply pipes.

**Feed concentration:** Feed concentrations varied between 5 and 15 wt%. To keep the material usage as low as possible the upper range of feed concentration was chosen at 15 wt%.

**Outlet valve trigger:** The power demand of the rotor and the resulting opening of the outlet valve were adapted to the feed concentrations and started at 12% of the overall performance of the rotor. This value for triggering the outlet valve was given by the minimum of power demand necessary to achieve at least a retentate. The upper range value had to be set way below the maximal capacity of the DynoTest (550 W), to prevent filter blocking and was chosen to be 16%. The discharge of the retentate at higher values was more difficult, since higher viscous slurries tend to block the valve. Blocking the outlet valve means that the bulk concentration inside the chamber increases while simultaneously the pressure increases as well. This resulting pressure increase might cause membrane damage. Values of the set-point, until it starts to triggering the outlet valve, varied between 12 % and 16 % (38,5 W - 88 W).

**Rotor speed:** The performance range of the DynoTest's rotation speed of the rotor is 600 and 1450 rpm. The operating range for the rotation speed of the rotor was chosen to be between 800 rpm and 1500 rpm.

Output parameters were:

- 1) residual moisture
- 2) permeate flux
- 3) temperature
- 4) chamber pressure
- 5) time to first opening of the outlet valve.



Taking all controllable factors into consideration a total number of 19 experiments had to be conducted.

The set up of the working package is shown in Figure 21. The run order is given by Modde with the goal to prevent systematic and operator errors.

Pressure [bar]	Rotor Speed [rpm]	Pump Speed [rpm]	Membrane [ $\mu$ ]	Model Substance	Feed concentration [wt%]	Rotor charge [%]
uncontrolled	800	300	0,05	Lactose	5	12
uncontrolled	1500	300	0,05	Lactose	5	12
uncontrolled	800	1500	0,05	Lactose	5	12
uncontrolled	1500	1500	0,05	Lactose	5	12
uncontrolled	800	300	0,05	Lactose	15	12
uncontrolled	1500	300	0,05	Lactose	15	12
uncontrolled	800	1500	0,05	Lactose	15	12
uncontrolled	1500	1500	0,05	Lactose	15	12
uncontrolled	800	300	0,05	Lactose	5	16
uncontrolled	1500	300	0,05	Lactose	5	16
uncontrolled	800	1500	0,05	Lactose	5	16



#### Input

- Pressure (uncontrolled)
- Rotor Speed
- Pump Speed
- Membrane (constant)
- Model substance (constant)
- Feed concentration
- Rotor charge

#### Output

- Residual moisture
- Temperature
- Permeate flow-rate
- Chamber pressure
- Time until first opening

Figure 21: Run order DoE 1

After performing the experiments statistical model correlating the input and the output parameters was designed with the target to find out which parameters are correlating with the residual moisture. The evaluation was done by Modde using following equations.

Out of the information of DoE 1 a set up to examine further impacts, such as properties of the model substances could be created.

### 3.5. DoE Evaluation

#### Regression analyses $R^2$

$R^2$  is the fraction of the variation of the response explained by the model, so that data of  $R^2$  determine how well the current runs can be reproduced. In consequence it overestimates the goodness of the fit. Modde calculating values of  $R^2$  by using following equation

$$R^2 = \frac{SS\ REG}{SS}$$

Equation 14

Where: SS REG = the sum of squares of Y corrected for the mean, explained by the model.  
SS = the total sum of squares of Y corrected for the mean.

#### $Q^2$

$Q^2$  is an index of the suitability of the chosen model, in other words,  $Q^2$  is an indicator how well the chosen model can predict new experiments. For calculations of the fraction of the variation of the response predicted by the model Equation 15 is used.

[20]

$$Q = 1 - \frac{PRESS}{SS}$$

Equation 15

Where: PRESS = the prediction residual sum of squares  
SS = the total sum of squares of Y corrected for the mean

Values of  $Q^2$  usually vary between zero and one. Values close to one, for both adhere explained statistical values, represent predictive models. On the other hand

values close to zero, or negative values of  $R^2$  and  $Q^2$  characterize very poor models. [20]

### **Model validity**

The Model Validity could be calculated, depending on the use of statistical test, as follows

$$\text{Model Validity} = 1 + 0.57647 * \log (\text{plof})$$

**Equation 16**

Where: “plof” = p for lack of fit

Inhere the Model Validity is based on the F-Test, and compares the model error of the pure error from the measured data. The declaration of the model Validity is again a declaration of how well a model fits. Model validity should at least reaches a minimum value of 0.25, the closer the value reaches the value one, the better is the fit of the model. [20]

### **Reproducibility**

The Reproducibility compares the variation of the responses under same conditions. During experimental working, this is mending by centre points. If there is no variation observed during repeating the experiments three times the Reproducibility should receive a value close to one. [20]

$$\text{Reproducibility} = 1 - \frac{MS_{\text{pure error}}}{MS_{\text{total SS corrected}}}$$

**Equation 17**

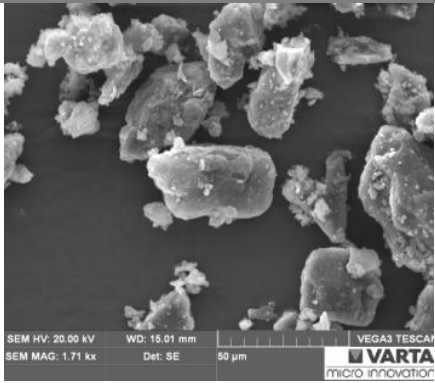
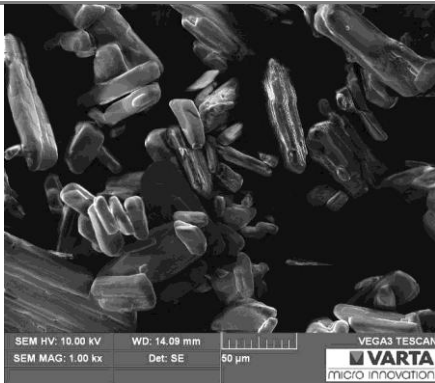
Where: MS = mean squares, or variance

## 4. Materials and Methods

### 4.1. Materials

The selection of the API (active pharmaceutical ingredient) was based on following criteria:

- particle shape and size
- particle structure
- surface modification
- melting point
- costs.

Material Company	Powder and particle characterization	SEM Picture	Physical properties
<b>Lactose</b> MEGGLE (Germany)	Granulac 230. Monohydrate crystals. Flow able powder. Shape: Cubes.  It is an ideal feed for studying a filtration system, because it is easy to prepare, and low in costs.		Solubility in water: 180 g/l at 20°C Hydrophilic
<b>Ibuprofen</b> BASF (Germany)	Ibuprofen 25. Shape: Voluminous needles. Poorly flowing powder.  Tends to form agglomerates, causes an accelerated sedimentation.		Solubility in water: 0,21g/l at 20°C  Hydrophobic

**Table 2: Materials overview**

**Additions: Isopropyl alcohol:** VWR (France) for technical usage.

**Sodium pyrophosphate tetrabasic:** Aldrich chemistry with a purity of  $\geq 95\%$ .

Other impacts, such as the formation of flocculates and consequently the sedimentation behaviour were taken into consideration. Pre-test were done to examine particle-particle interactions and solubility. The general operation procedure was to prepare a saturated mother liquid followed by the addition of the API, till a certain concentration was reached. Distilled water was used as mother liquid. Table 2 shows an overview of the used materials and their properties.

### **Lactose**

The Lactose suspension tested had a mean particle size of 33.69  $\mu\text{m}$ . It is an ideal feed for studying a filtration system, because it is easy to prepare, and low in costs. The Lactose powder (Granulac and Sobulac) was bought from the Meggle Wasserburg Company (Germany). The particle size distribution was determined and is shown for both tested particle sizes in Table 3.

### **Ibuprofen**

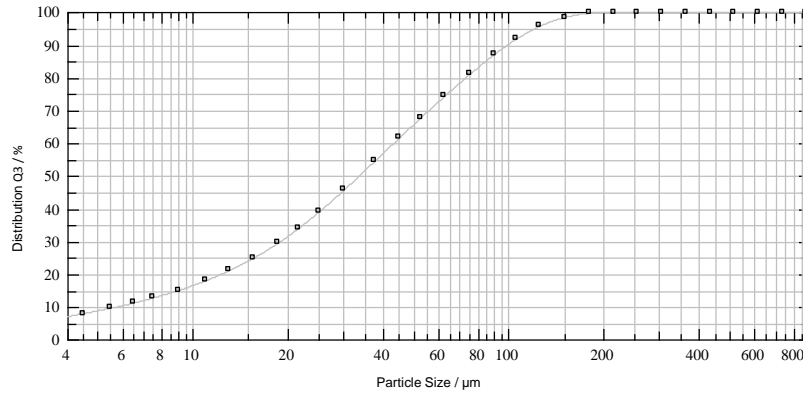
The Ibuprofen suspension tested had a mean particle size of 51.60  $\mu\text{m}$ . The Ibuprofen powder was bought from the BASF Company (Germany).

During the pre-test the build up of flocculates was observed, affecting an accelerated sedimentation. Furthermore the hydrophobic surface causes a more difficult suspending of the API in water. To counter act these effects 0.08 wt% of Sodium-pyrophosphat-tetrabasic were pre-dissolved in distilled water. Sodium-pyrophosphat-tetrabasic was used to stabilize the suspension. The addition of Ibuprofen was done slowly, to minimize the built up of flocculates. Ibuprofen was used as model substance during the washing studies.

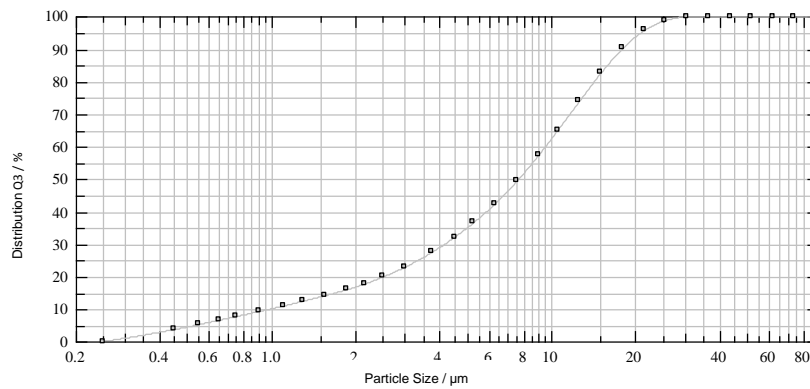
The particle size distribution of Ibuprofen 50 is shown in Table 3.

Material	Particle Size Distribution
----------	----------------------------

<b>Granulac</b>	$X_{10} = 5.78 \pm 0.02 \mu\text{m}$
	$X_{50} = 33.69 \pm 0.29 \mu\text{m}$
	$X_{90} = 99.47 \pm 0.75 \mu\text{m}$



<b>Sorbulac</b>	$X_{10} = 0.99 \pm 0.01 \mu\text{m}$
	$X_{50} = 7.61 \pm 0.04 \mu\text{m}$
	$X_{90} = 17.84 \pm 0.12 \mu\text{m}$



<b>Ibuprofen 50</b>	$X_{10} = 15.27 \pm 0.50 \mu\text{m}$
	$X_{50} = 51.60 \pm 0.74 \mu\text{m}$
	$X_{90} = 121.44 \pm 0.62 \mu\text{m}$

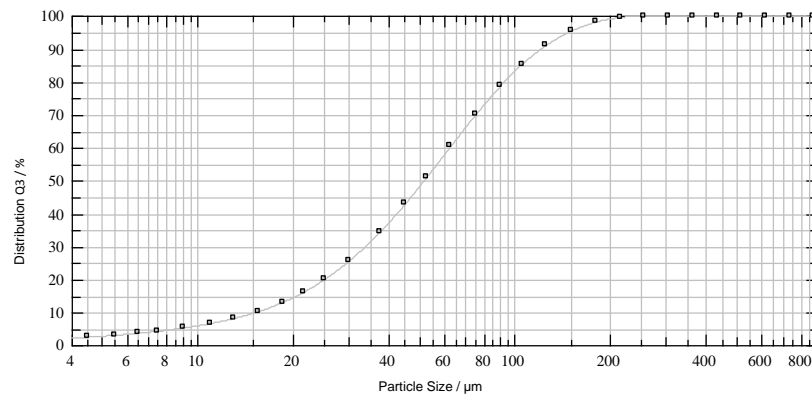


Table 3: Particle Size Distribution

## 4.2. DynoTest

The DynoTest is based on the principle of a dynamic shear gap filter. There is a propeller placed in front of the membrane, which generates the cross flow and enhances the turbulent flow in the filtration chamber. Figure 22 shows the DynoTest with open front panel. Depending on the rotation speed of the propeller, the build up of a filter cake is kept on a minimum, resulting in a maximum reachable permeate flow- rate.

The pump delivers the suspension into the filtration chamber. The power demand of the rotor shaft increases proportionally with the increase of solids' concentration inside the chamber. The discharge of the retentate can be controlled by means of the required power demand of the drive. The outlet valve opens when a certain, free adjustable set- point is reached and discharges the retentate at the desired concentration.

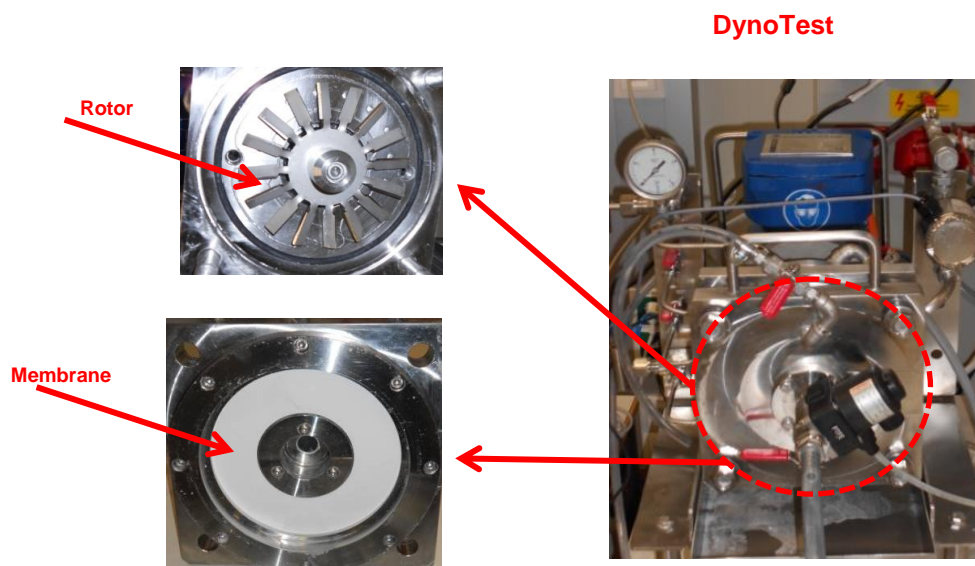


Figure 22: Transportable lab filter for cross flow filtration; DynoTest

Design specifications for the tested equipment are:

- filter area: 130 cm<sup>2</sup>
- diameter of agitator: 140 mm
- max. filtration pressure: 7 bar abs.
- dimensions: L x W x H = 520 x 510 x 330 mm
- weight: approx. 40 kg
- depth of chamber: 22-30 mm (variable)
- adjustable gap to agitator: 3-5 mm

Process Flow Sheet

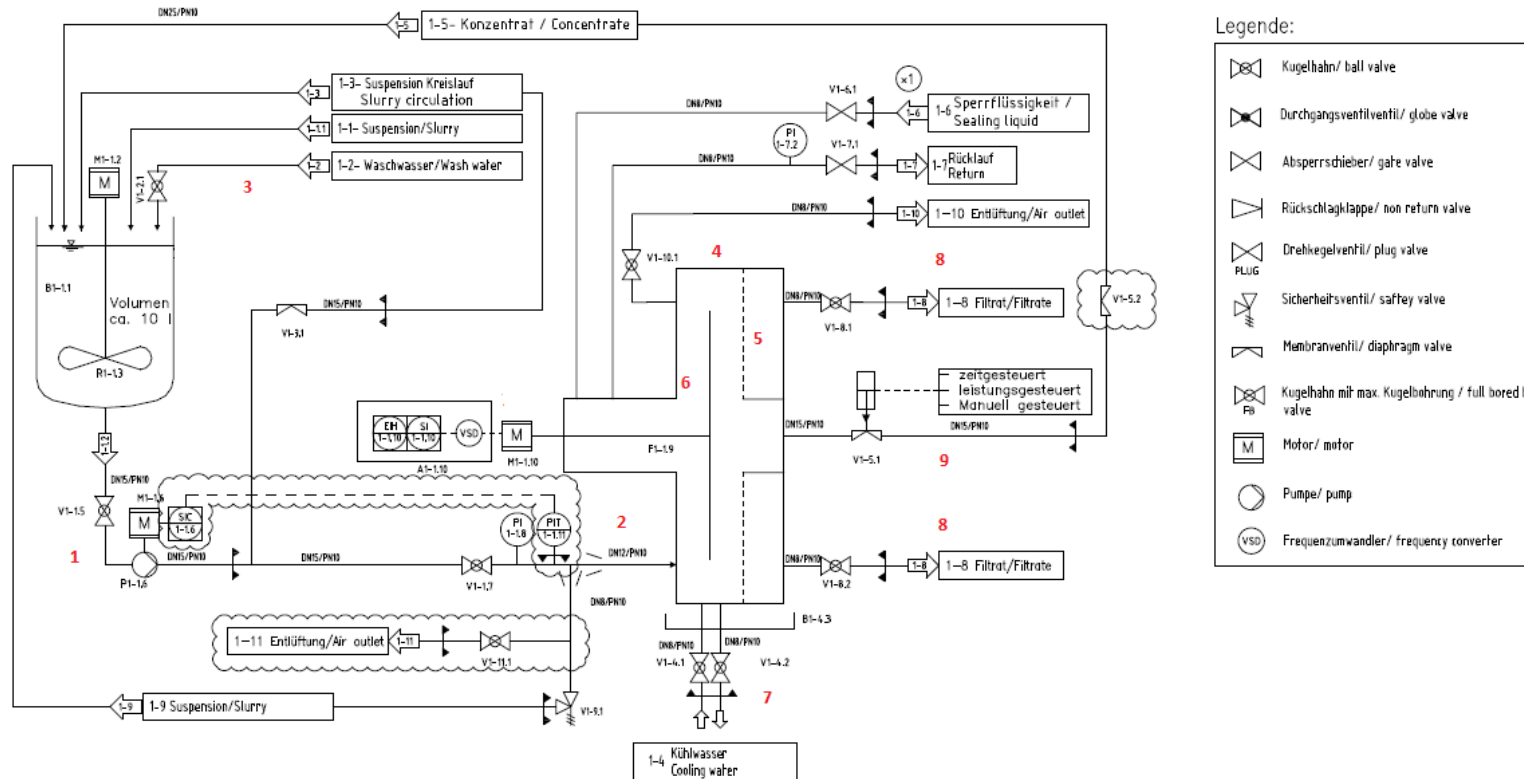


Figure 23: Process Flow Sheet



---

**Brief description of the flow sheet**

(1) Feeding unit	The feeding unit is a progressive cavity pump with a range of 0:3 to 120 L per hour, and could be controlled separately
(2) Inlet for suspension feed	Fluid feed products can be pumped into the DynoTest; a pressure-side manometer (PI 1-1.8) is installed
(3) Inlet wash water	Wash water could be pumped through the storage tank, or separately delivered by a recirculation valve (1-7)
(4) Filter	The filter has a filled volume of 0.36 L and a filter area of 0,13 m <sup>2</sup>
(5) Membrane	0.05 µm PTFE Membrane
(6) Motor	The motor M1-1.10 for the filter is driven by a frequency converter; The rotational speed range is from 0-1405 U/min (frequency range 0-50 Hz).
(7) Cooling system	The filter of the DynoTest is water cooled.
(8) Outlet of the filtrate	There are two additions of an outlet valve on the top plate, used for filtrate discharge.
(9) Pneumatic membrane valve	The pneumatic valve can operate in three different ways. Torque, time and hand controlled.

---

**Table 4: Flow Sheet Description**

Table 4 describes the different units of the whole process. As shown in the flow-sheet the suspension is stirred in the vessel. A progressive cavity pump (1) delivers the suspension into the filtration chamber (2,4) where the rotor generates the turbulent flow (6). Friction heat is dissipated by the cooling system (7). The permeate can be removed by outlet valves (8). After reaching a certain concentration, the retentate gets discharged by the pneumatic membrane valve (9). There is the possibility to recycle the retentate by another valve; this is done when the required residual moisture is too high.

---

#### 4.2.1. DynoTest Principle Process Description

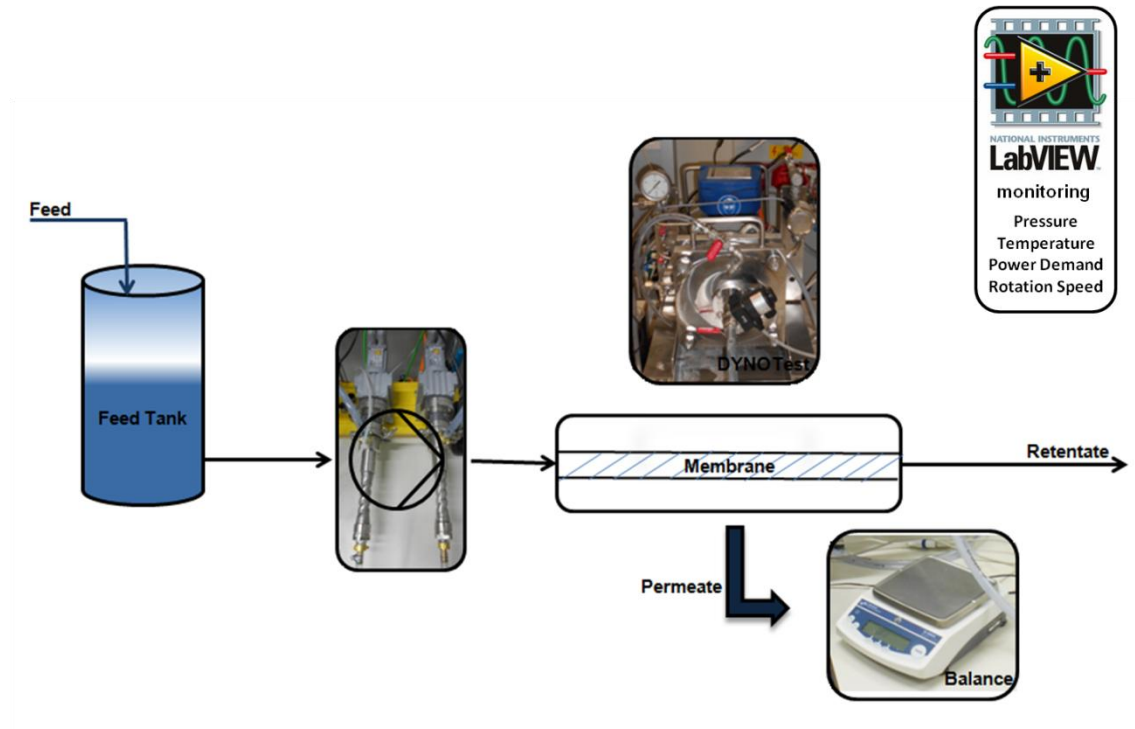


Figure 24: Process Description

Following tasks had to be done before performing the DoE runs. The membrane needed to be completely wetted to guarantee a successful performance of the experiments. This was done by using de-ionized water. As a next step, all supply pipes and the filtration chamber were ventilated from air, by feeding de-ionized water through the system until it was air-bubble free. Then the cooling system was switched on so that cooling water was circulating in the filter housing to prevent temperature gradients (cooling water pressure was set to 1.5 bar). At least the membrane was washed inside for one hour, by feeding de-ionized water through the filtration system. The feed rate was kept low (resulting feed pressure was 1 bar) and the outlet valves were kept open to get rid of material impurities, which might affect the process. To avoid the rise of negative pressure, the rotor was switched off during each preparation step.

To start-up the DynoTest, all outlet valves were closed, and the rotor was switched on. The slurry was fed through the supply pipes into the filtration chamber, and the outlet valve of the permeate flux was opened. Due to the

ongoing discharge of the permeate flow-rate the solid concentration inside the filtration chamber rose, as well as the viscosity. In consequence the power demand of the rotor increased as well as the pressure increased. At the same time the total flow resistance was enhanced due to particle deposition on the membrane. After reaching the predefined set-point of the power demand of the rotor, the outlet valve of the retentate opened, and the high viscous slurry was discharged. This point in time indicates the change of the operation mode. In steady state the operation mode changed from batch to constant filtration. While the outlet valve of the retentate stayed open, the solid concentration inside the filtration chamber decreased, resulting in a decrease of the power demand of the rotor. This is when the outlet valve of the retentate closed again.

Under ideal conditions the discharge of the retentate and the permeate was equal to the amount of the slurry fed inside the filtration chamber. Thus, the incessant triggering of the outlet valve of the retentate indicated the steady state, during the experiments the steady state was initialized manually. This was done by keeping the outlet valve of the retentate open as soon as the change between batch and constant power demand was detected.

In practice, the trigger for valve opening would have to be set for a viscosity level slightly higher than the viscosity of the desired final concentration. This should be done to avoid the effect of the drop in viscosity during the outlet valve stays open.

#### **4.2.2. The control system of the DynoTest**

The DynoTest can be controlled by a panel mounted in front of the control cabinet, shown in Figure 25. The rotation speed of the propeller can be regulated within a range of 600 to 1450 rpm (7). The pneumatic valve can operate in three different ways, rotor load/ rotor power capacity controlled, time and hand controlled (10). The limit of the power capacity of the rotor can be preset. The limit of the power capacity is calculated by a percentage value of the overall performance of the motor, which is 550 W. (e.g. the predefined

set-point of 30 % means that 30 % according to the overall performance of 550 W) The valve opens when the free adjustable set-point is reached and closes at the end of the predefined period of time. The opening interval can be manipulated via two timers mounted on the control cabinet, at the position 11 and 12. The opening interval and the time span can be variable changed. The pneumatic membrane valve can be opened manually too. This is an important aspect during dial filtration. During dial filtration the concentrate was recycling, simultaneously the filtrate discharged. When a certain concentration in the receiver tank is reached, the addition of wash water can be done and kept at a constant filling level (amount of wash water = amount of discharged filtrate).

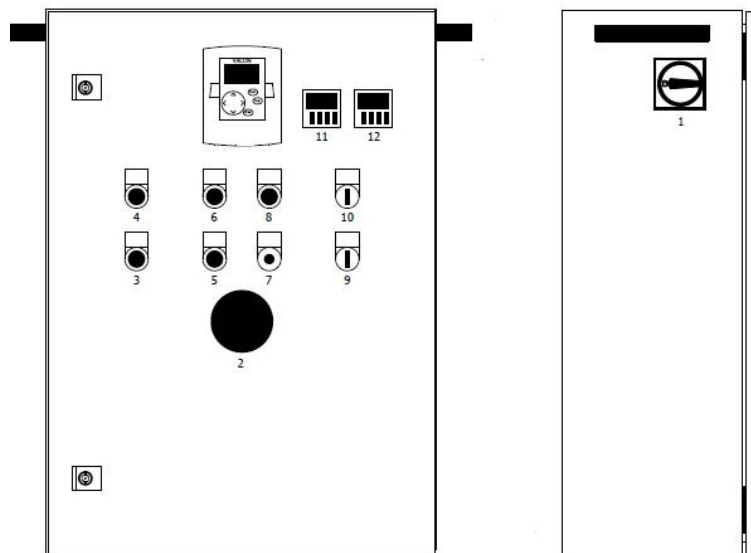


Figure 25: Control system

1 main switch; 2 emergency shut down; 3 and 4 control power off/on; 5 and 6 filter power off/on; 7 rotational speed; 8 filter failure; 9 dissipation (on/off); 10 torque / time / hand controlled; 11 opening intervals; 12 opening time

#### 4.2.3. The LabView control panel

Pressure, temperature, rotation speed and rotor power demand monitoring was done via LabView. LabView is shortened for Laboratory Virtual Instrumentation. With this software engineering workbenches within system design platforms

could be generated. It is based on visual programming and therefore simple in use. It is possible to connect several process controllers and systems in one virtual instrument (VI). So far, pressure, time, rotation speed and rotor power demand were collected using only one VI shown in Figure 26.

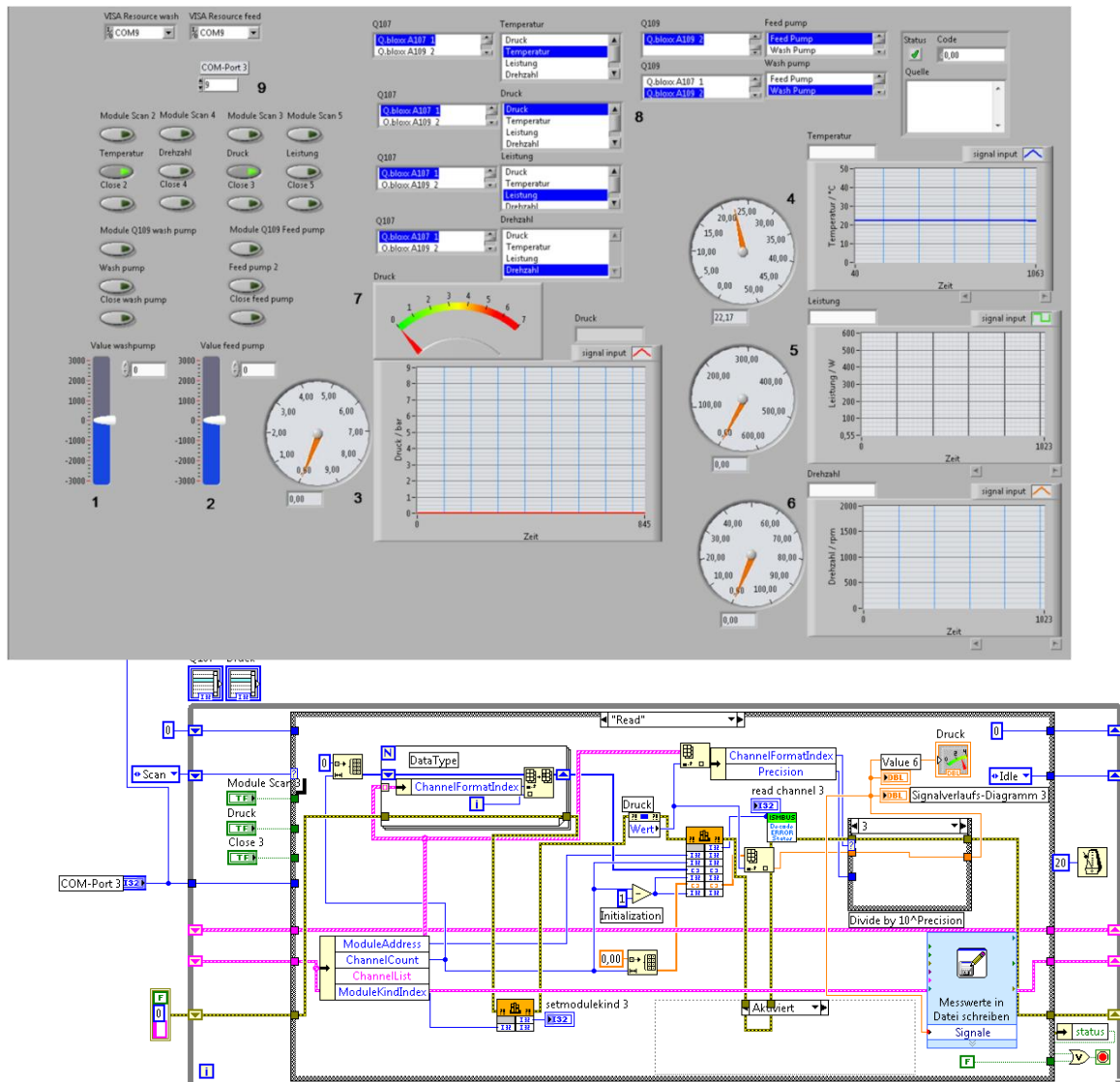


Figure 26: Working bench LabView

## 5. Measurement Methods

### Residual moisture

The residual moisture of the retentate was detected using thermogravimetry analysis. The slurry was dried for a period of maximum 48 hours in the drying chamber to constant mass. Drying temperature was set to 80 °C for Lactose and 60 °C for Acetanilide and Ibuprofen. The mass of the dry solid was then determined by weighing using a balance (Model SI - 4002A). The water content of the retentate what is the residual moisture can be calculated by simple mass balance.

$$\text{residual moisture} = \frac{(\text{mass of retentate}) - (\text{mass of dry solid})}{(\text{mass of retentate})}$$

Equation 18

### Permeate flux rate

The average filtration rate was calculated by weighing the permeate flux using a Denver Summit balance (Model SI - 4002A) with an increment of 10 mg. The increase of the flux rate was monitored via a RS232 port every second. Data were exported in an Excel-Sheet and the average filtration rate was then calculated by linear approximation.

### Retentate flux rate

During processing the retentate was collected in a basin. The amount of retentate was weight. Retentate was then calculated by dividing the amount by the process time.

$$\text{Flux rate} = \frac{\text{material collected in the basin}}{\text{production time}}$$

Equation 19

**Temperature**

The temperature was measured using a resistance thermometer (Pt 100 DIN EN 60751 KI 0.15/0 °C). All data were collected via LabView. The thermometer was placed in the product discharge supply pipe, right after the outlet valve.

**Pressure**

The pressure was measured via a pressure transducer by ABB, model 261GS flush-mounted and ATEX Ex nA IIC T6 prove (base accuracy:  $\pm 0.1\%$ ; span limits: 0.3 to 60000 kPa; 1.2 in H<sub>2</sub>O to 8700 psi; 4 to 20 mA output with HART communication as standard; Conforms to SIL2 acc. to IEC 61511; Full compliance with PED Category III). The pressure transducer was placed in the feed supply pipe, right in front of the inlet valve. This pressure was detected as the average chamber pressure. All data were collected via LabView.

**Time detection**

Time measurements were done by using the internal clock of the PC connected to the feed pumps. The time detection started as soon as the feed pumps were initiated.

**Rotor speed**

The rotor speed was sourced out of the control system implemented by Bokela. The present value was calculated by linear correlation between the frequency of the rotor motor and the rotor speed ( 50 Hz equals approximately 1450 rpm).

**Rotor load / power demand**

Also the power demand of the rotor was sourced out of the implemented control system by Bokela. The value of the rotor load was calculated using data out of the frequency converter. These given values were of approximate nature. A deviation was be expected especially at lower power capacities. General trends still could be easily deduced.

## 6. Experimental Work

### 6.1 Preliminary Experiments

Calibration of the feed pump was done to guarantee gradient free delivering of the slurry. Pre- studies, according to feed-rate, feed concentration and rotor-load triggering, were done to define feasible values of the factors. Furthermore to get an overview of the DynoTests handling several initial amounts of slurries were tried out to filtrate.

#### 6.1.1. Feed Rate Calibration

The progressive gravity pump (by SEW) shows a feeding range of 0.3 up to 120 L/h. In between this range calibration studies were done first. For that water was pumped through the feeding unit within a predefined time-span. Seven measurement points (100, 200, 600, 800, 1000, 1500, and 2000 rpm) were chosen and the flux was measured for 10 minutes and extrapolated to one hour. The mass of received water was weighted and the mass feed rate could be calculated as follows. For calibration, this procedure was repeated five times.

$$\text{mass feed rate} = \frac{\text{mass of material in the bucket}}{\text{runtime of the feed}} * 60$$

Equation 20

Figure 27 shows the calibration curve.



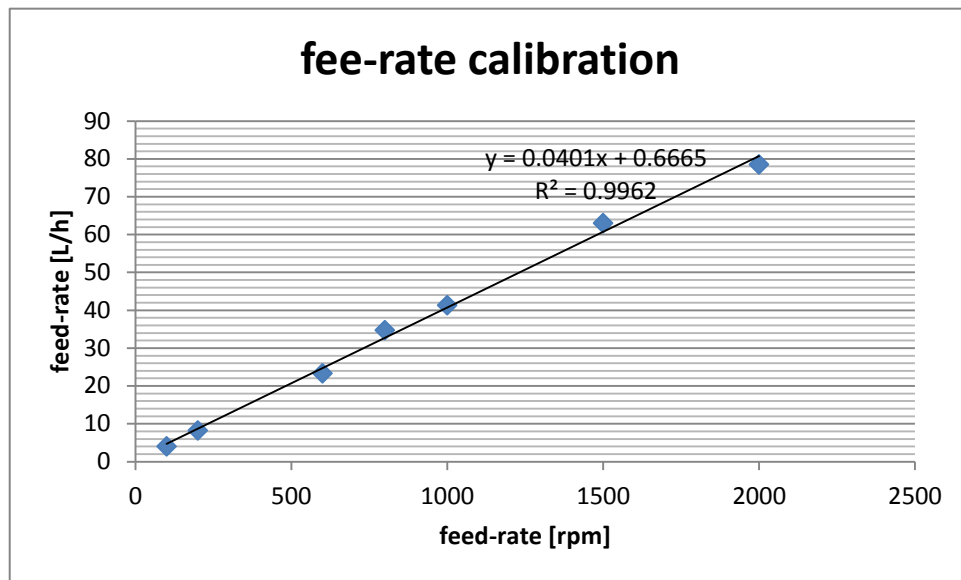


Figure 27: Calibration of progressive cavity pump

### 6.1.2. General Start Up Experiments

To gain more information of critical process parameters preliminary experiments had been conducted. Critical process parameters were **rotor-load triggering**, **feed-rate** and **the amount of suspension to be filtrated**. The maximal feed concentration was already predefined to be 15 wt%. These preliminary tests were processed with Lactose, as it is easy to process and low in costs.

In early studies smaller **amounts** of 2 L were tested, showing unsatisfactory results. Bokela states that a minimum of 2 L suspension is still filtrateable. Theoretically this should be possible by recycling the retentate, which is not entirely true. During processing with this small amount of suspension, finding a useful set-point for triggering of the outlet valve was not realizable. As a consequence, solid contents reached during recycling the retentate was nearly the same as the initial concentration of the suspension. Since one of the goals is to reach steady state conditions under batch processing, the minimum on amount of suspension was chosen to 7 L.

**Feed-rate** is correlated with the pressure building up in the filter chamber. This chamber pressure should at least not exceed 4 bar. Depending on the feed

concentration feed-rates between 13 L/h and 73 L/h could be handled. To remember, an increase in solid content causes an increase in chamber pressure.

The set point of the **rotor-load triggering** has an impact on residual moisture, and should therefore be as high as possible. First set-points were varied between 30 % and 50 %, while the feed concentration was 20 wt%, this was ending up in a blocking of the membrane. For lower feed concentration, less than 5 wt%, no retentate was received. Figure 28: Blocking of the filter shows the blocking of the membrane while the set point of the outlet triggering was 30 %. It was observed, that the transition between incessant filtration and blocking the membrane happened nearly spontaneously. The transition-point was characterized by a quick increase in power demand of the rotor. At the same time hindered rotation of the propeller until the propeller got stocked was observed. As a consequence the rotor load triggering should not exceed the value of 13%.

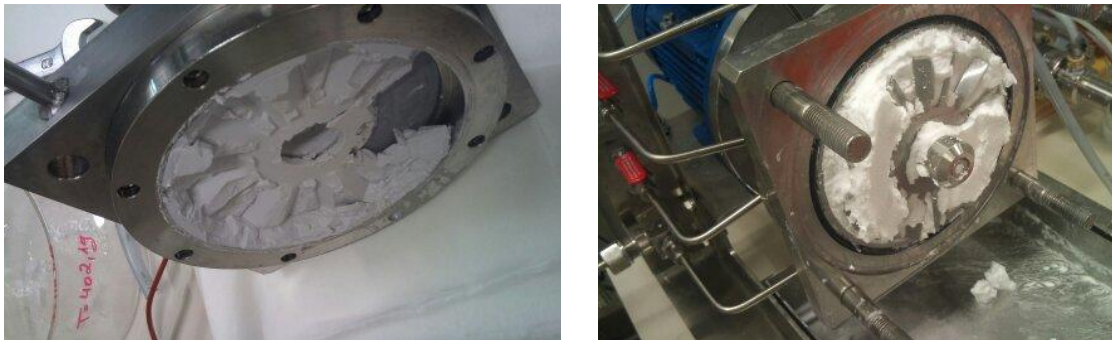


Figure 28: Blocking of the filter

In conclusion of this short experiment it can be said, that the use of rotor load triggering cannot be exhausted for reaching very low residual moisture. The challenge is to discharge this high viscous slurry, which was not possible without blocking the filter. Therefore the outlet valve triggering was kept at a low

level. Table 5 shows an overview of values of rotor load triggering until the discharge of the retentate is still feasible.

Rotor load [%]	Lactose discharge
7	Yes
9	Yes
10	Yes
13	Yes
15	Yes
17	Only with high pressure
19	Only with high pressure
22	Only with high pressure

**Table 5: Rotor charged discharge**

## 7. Results and Discussion

This section covers the evaluation of the raw data, as well as the statistically evaluated predictions that were based on Modde, especially with regards to residual moisture. It was tried to link the responses to their impacts and a comprehensive audit procedure that summarizes all the previous outcomes will be presented through the following chapters.

Evaluation will be primarily done based on pressure data and compared against each other so that rise and fall of pressure could at least indicates high or low values of residual moisture. Modified process parameters are listed, compared and evaluated according to their influences on residual moisture and permeate flow-rate respectively.

In here, only statistically significant results are presented. Experiments not yielding any retentate were neglected.

The aim was to generate useful information about process conditions based on the prediction of the future robustness or capability of the DYNOTest, and to be able to obtain a subsequently performed set up of experiments with regard on the influences of the model substance on the investigated system.

Also preliminary washing experiments were preformed and are going to be discussed within the following chapters. Their comparison referred to their kind of operation mode, if the washing agent was added batch-wise or ongoing. These experiments were carried out strictly as a feasibility study and serve mainly as a basis for subsequent experiments which will deal with the exchange of mother liquid within the final filtration process.

## 7.1 Raw data Evaluation – Residual Moisture

Table 6 shows the process impacts, and their variation through the experiments, while Table 7 presents the resulted and measured values out of the DoE.

Only a third of conducted experiments provide data for residual moistures, varying between 27 to 72 %. Other experiments yielded no retentate.

Experimental Number	Feed Rate [rpm]	Rotation Speed of the rotor [rpm]	Feed Concentration [wt %]
DoE1_2_N4_2	41-7 L/h	1500	5
DoE1_2_N17	37-13 L/h	1500	10
DoE1_N9	7 L/h	1500	15
DoE1_N11	7 L/h	1500	15
DoE1_N12	73-37 L/h	1500	15
DoE1_N13_3	19-13 L/h	1500	10
DoE1_N15	23 L/h	1500	15
DoE1_N15_2	19-13 L/h	1500	15

Table 6: Process Impacts



Experimental Number	Residual Moisture [%]	Permeate Flux [kg/h]	Chamber Pressure [bar]	Rotor Load Triggering [%]
DoE1_2_N4_2	57.5	6.75	4.0	12
DoE1_2_N17	26.5	13.17	5.0	14
DoE1_N9	51.6	7.65	0.4	16
DoE1_N11	41.7	5.88	1.3	16
DoE1_N12	34.0	46.02	4.0	16
DoE1_N13_3	50.4	3.60	2.0	16
DoE1_N15	69.1	2.19	0.9	16
DoE1_N15_2	71.8	4.47	0.7	16

Table 7: Process Responses

### Effect of the outlet valve triggering on residual moisture

The opening of the outlet valve was controlled by the power demand of the rotor, corresponding to the viscosity increase of the bulk. The viscosity increase of the bulk was resulting out of the increase in solid concentration within the filtration chamber. By exceeding a pre-defined set-point (12-14-16 % according to the overall power consumption of the rotor) the outlet valve was triggered. From that point on, the bulk concentration should be kept constant.

Values of received residual moisture varied between 27 up to 72 %, even at same set points. This brought distribution in water content is a consequence out of the mechanical arrangement of the DynoTest. Due to this arrangement, deposition and sticking of the bulk onto the rotor shaft and the rotor blades was observed. As a consequence the removal of water was different, depending on the preferred location of deposition. Figure 29 shows a cross-section through the DynoTest and the location of solid deposition.

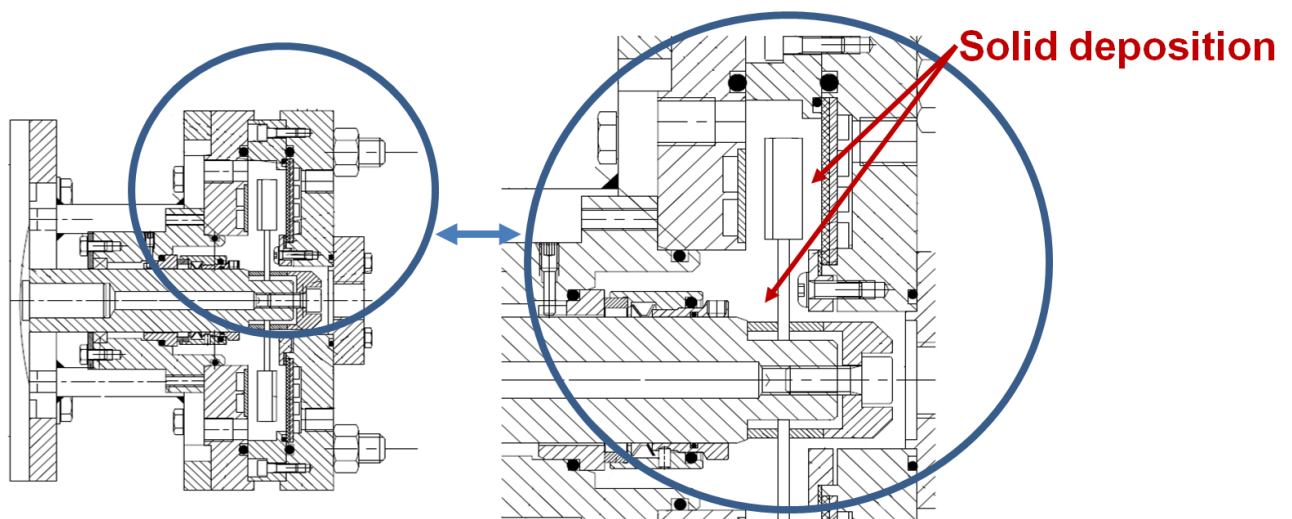


Figure 29: Solid deposition inside the filtration chamber; cross section

Permanent bulk deposition and removal onto the rotor shaft and the rotor blades caused huge fluctuations in power demand. Once bulk was deposit, the power demand was increasing, by shearing of the bulk in between the blades and the shaft of the rotor, power demand was decreasing again.

### Effect of the pressure on residual moisture

As expected, the influence of the chamber pressure on residual moisture was huge. According to Darcy's Law, pressure is increasing proportional to permeate flow-rate when the flow resistance is kept nearly constant.

$$J = \frac{\Delta p}{R * \mu}$$

Equation 21: Darcy's Law

Consequently, the residual moisture was decreasing with increasing chamber pressure.

Pressure increase within the filtration chamber was observed at

- high rotor load set points
- high feed concentrations
- high feed-rates.

The relationship between rotor load depended opening of the outlet valve and the pressure increase was given by the increase in bulk concentration inside the filtration chamber. The later the outlet valve opened, the more suspension was fed into the filtration chamber so that bulk concentration is increased as well as flow resistance. As a further consequence, bulk dwelling was increased, and lower values of residual moisture could be achieved.

The effect of feed concentration on pressure was again caused by the increased bulk concentration. Higher initial solid concentrations led to an increase of chamber pressure, due to the fast increase of the bulk concentration. This effect on pressure might not be seen by raw data evaluation, because it is correlating to the feed rate. At lower feed rate a lot of solid sedimentation was observed within the supply pipes. This loss in solid content led to less pressure increase inside the filtration chamber. The effect of feed concentration on pressure was therefore more significant at higher feed rates.

The observed pressure increase at higher feed rates was much faster when filtrating suspension including 15 wt% Lactose. In some cases it was even necessary to throttle the feed rate due to exceeding the maximal permissible pressure. The maximal permissible pressure is 5 bar, this is when the safety valve opens. This fast and huge pressure increase suggests that a deposition of a concentration boundary layer onto the membrane occurred, even at those high shear-rates. This deposition caused over and over again a blocking of the membrane. Consequently the flow resistance increased and led to even higher pressure increases. This assumption was confirmed by comparing the feed-rate with the permeate flux. As explained in chapter 2.2., the deposition of a concentration boundary layer should be reversible. If the feed-rate once had been interrupted, pressure was decreasing while the permeate flux was increasing again.

Figure 30 shows the decrease in permeate flux over time. It is shown that by increasing the feed rate, permeate flux stays nearly constant over a period of five minutes. It is known that pressure decrease is induced among others by reducing the feed rate which in turn simplifies the off-shearing of the concentration boundary layer.

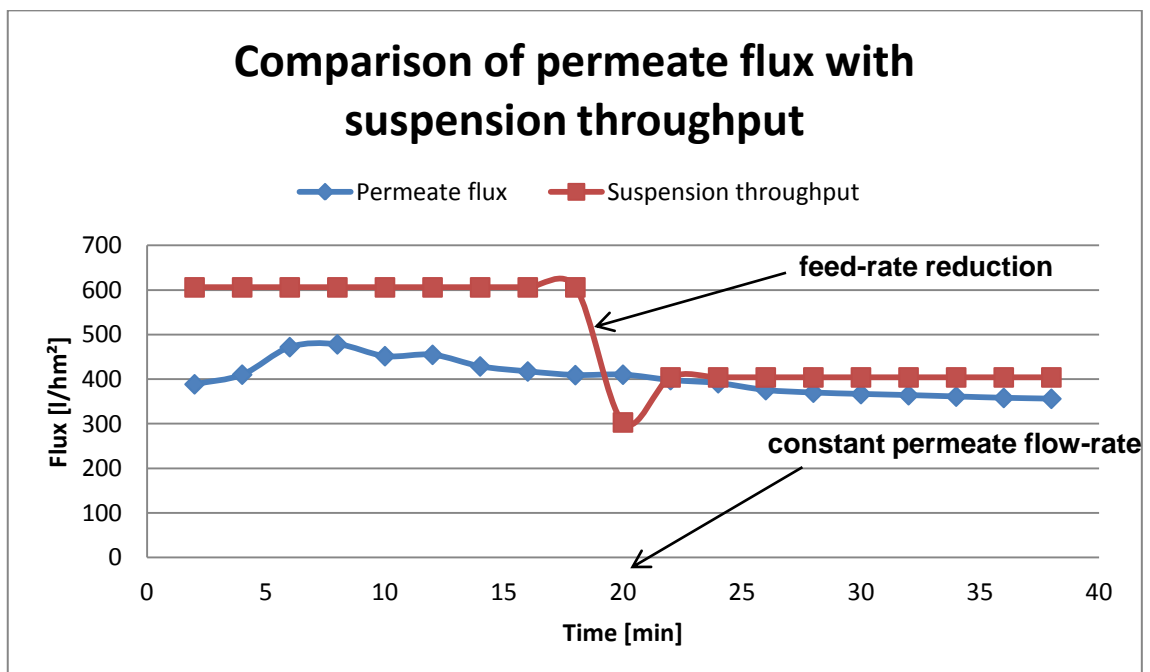


Figure 30: Comparison of permeate flux with suspension throughput



To summarize, the increase in pressure had a beneficial effect on residual moisture, since it decreased with increasing chamber pressure. Higher feed rates, higher feed concentrations and a delay in opening the outlet valve led to an increase in chamber pressure.

## 7.2. Statistical Evaluation - DoE

Statistical evaluation was done via Modde, by comparing the resulting data of responses with the factors. Proposed statistical models were evaluated and inhere discussed. Figure 31 shows the experimentally evaluated model performance indicator plot.

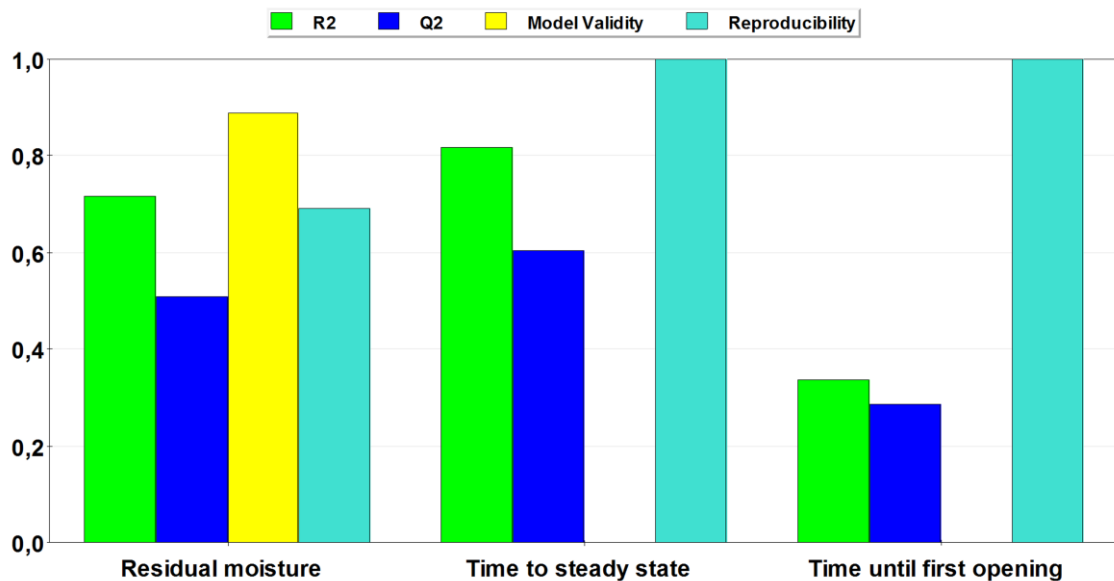


Figure 31: Performace Indicator Plot

The responses are plotted on the x-axis, and their magnitude of effect is plotted on the y- axis. At least only residual moisture is meant to be effected. Model validities of time to steady state and time until first opening the outlet valve showed a significant lack of fit of the model which was chosen. Model validity, as mentioned in the theory, should at least reaches a minimum value of 0.25, the closer the value reaches the value one, the better is the fit of the model.

Reproducibility ( $R^2$ ) is close to 0.7. Such a low value was already expected as received data of the center points experiments were varying. Values of  $Q^2$  should not fall below 0.5. In here one could say the chosen model represent a good predictive model. Nevertheless the values of Reproducibility and  $Q^2$  should not differ in more than 0.2 units. As it was expected, accordingly to the

lower value of model validity, in this evaluation, they differed close to 0.2, which indicated, that the chosen model was not perfectly fitted.

Figure 32 shows the pure coefficient plot for residual moisture.

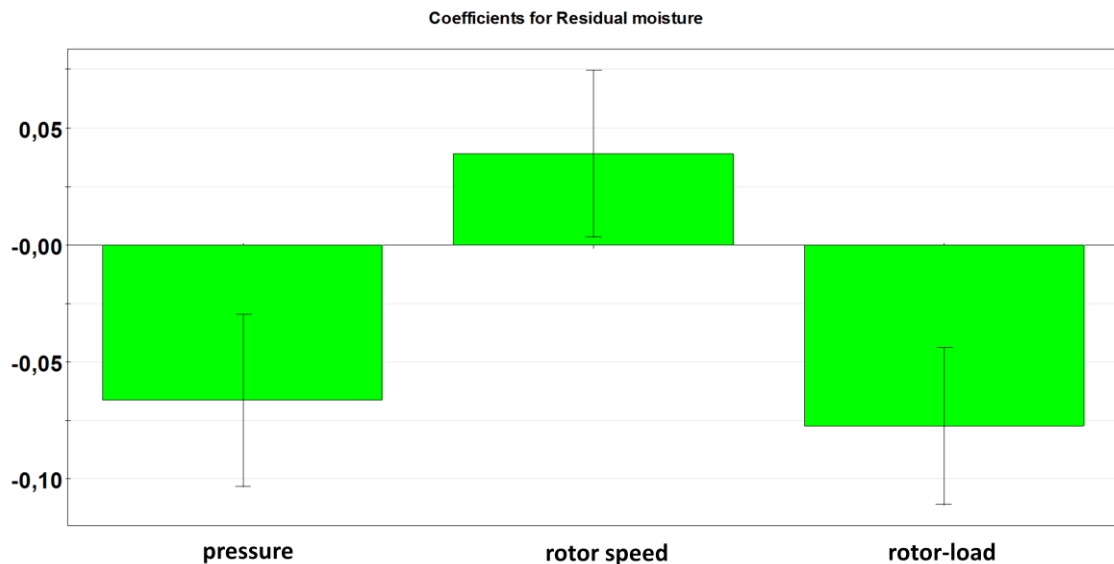


Figure 32: Coefficient Plot

In this plot only statistically significant factors with effects on residual moisture are represented. All other effects, wherein the model error was higher than the pure error of the data were eliminated to increase the quality of the model. Factors having statistically significant effects on residual moisture were pressure, rotation speed of the rotor and rotor-load triggering of the outlet valve. This prediction was in good agreement with the raw data evaluation. At least pressure was observed to have a huge impact on residual moisture. Even rotation speed and rotor-load triggering showed poor effects by comparing the raw data, it was expected that the real impact was much higher. Since the power demand of the rotor increased proportionally with the viscosity inside the filtration chamber, first opening of the outlet valve was controlled by that increase of concentration.

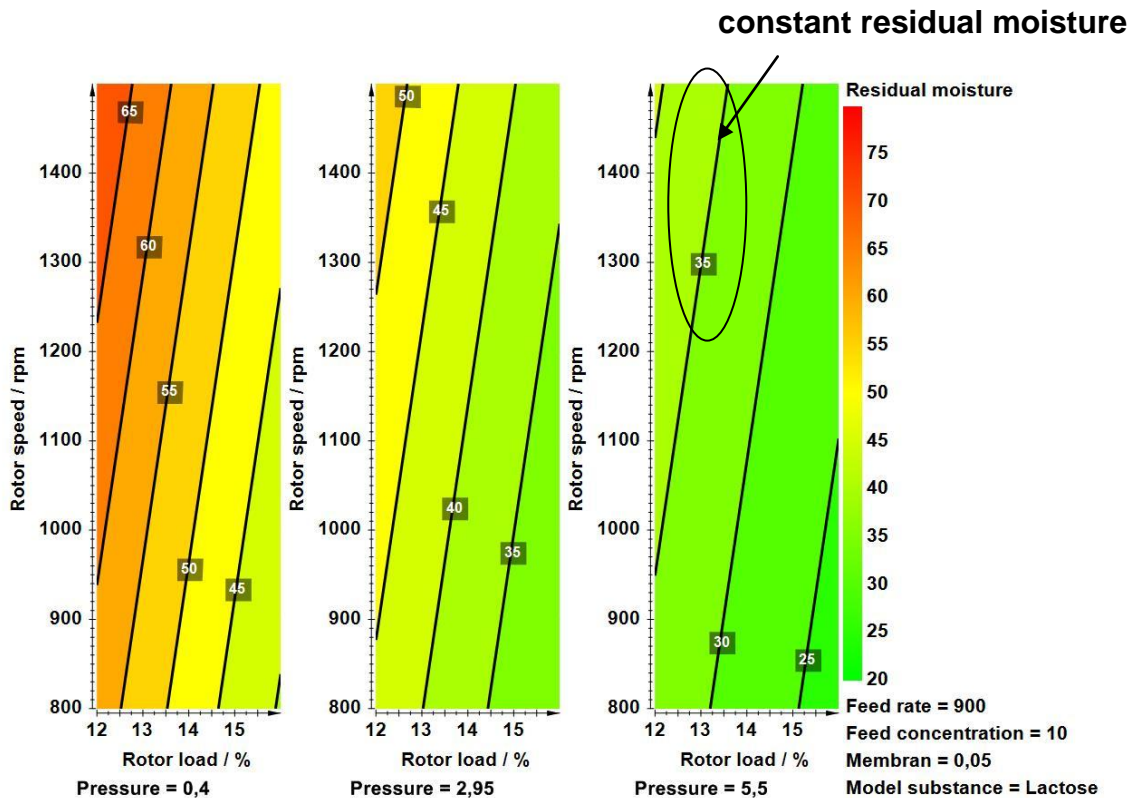


Figure 33: Counter Plot

Figure 33 shows the prediction of the model for residual moisture, using Lactose as model substance. The outer boundary conditions are feed-rate (900 rpm), feed concentration (10 wt%), membrane pore size (0.05  $\mu\text{m}$ ) and model substance (Lactose; Granulac). Along the lines the values of residual moisture are constant. At constant outer boundary conditions it is feasible to predict preferable residual moistures by choosing suitable values of the rotation speed of the rotor (y-axis) and values of power demand until first opening the outlet valve (x-axis).

## Summary

To summarize, raw data evaluation and statistical evaluation were in good compliance with each other. The main effects on residual moisture were:

- (1) chamber pressure
- (2) rotation speed

In fact, the increase of chamber pressure was a consequence out of higher feed-rates and feed concentrations as well as a delay in opening the outlet valve. On the other hand the increase of rotation speed of the rotor affected the shear rate positively, which led to a reduced deposition of particles. The decrease in shear forces could be affected by the rise in bulk concentration. The increases in viscosity affected inversely proportional the Reynolds number, resulting in less turbulences.

Even at high shear rates the build up of a concentration boundary layer was observed. This might be the effect of the decrease of the Reynolds-number due to viscosity increase. By reducing further on the rotation speed of the rotor, a build up of a filter cake will be a consequence out of the reduced shear rate. This leads to a significant loss of permeate and should therefore be avoided in the following experiments.

However as already mentioned, the huge and fast pressure increase was always a challenge during the performance of the experiments. This pressure increase could be a consequence out of several factors. The effect of the characteristic of a material, such as different substance shapes, size and chemical properties, made it more or less attractive for membrane blocking.

The observed fast increases in pressure within the fast decreases in permeate flux, indicates the membrane blocking. The particle size of lactose showed a distribution of 5 up to 100  $\mu\text{m}$ , whereas the pore size of the membrane has an average pore size distribution of 0.05  $\mu\text{m}$ , which means that theoretically only one larger particle could blockade at least 2000 pores. Now that particle deposition occurs the increase in pressure assisted the effect of membrane blocking and a highly viscous and compact gel on the membrane is the

---

consequence, and leads once to an increased flow resistance and furthermore to the mentioned membrane blocking.

This phenomenon is discussed in the theory in Chapter 2. Pressure decrease, followed by a decompression of the concentration boundary layer, will reduce particle deposition. As a consequence this concentration boundary layer can be sheared off.

It is suspected that due to the use of a hydrophobic membrane, precipitation of lactose within the pores of the membrane happened. This effect caused a fast and uncontrolled increase in pressure. To be able to start up the next experiment, it was necessary to wash the filter. While water was fed through the filtration system, pressure decrease was observed. In order to this it can be assumed that recrystallized lactose which was clogging the membrane has been washed out with water.

In summary, the DynoTest worked very well and achieved adequate values of residual moistures, by using high initial concentration, high feed rates, and high values of power demand depended opening of the outlet valve.

There is a need to adopt the membrane pore size to the particle size to minimize flow resistance and to optimize pressure distribution inside the filtration chamber. Alternative the material to be filtrated could be previously milled or any other grinding step could be used prior. The relationship  $1/10$  provides an optimum proportion rate. [3]

Feed-rate, as well, impacted predominant pressure on the membrane, and should at least, taken into consideration. Lower feed-rates cause concentration-gradients by the sedimentation of particles inside the supply pipes. Distances between receiver tank and filtration unit consequently should be minimized.

Power load demanded outlet valve triggering, was proposed to facilitate processing and to achieve constant product quality. This could be a useful tool if the concentrated slurry is just an intermediate step in between subsequent processing, where required residual moistures could be higher and doesn't afford constant water content.

To apply the discharge of the retentate a minimum pressure was required, depending on the solid concentration inside the filtration chamber. A higher viscosity of the slurry postulates a higher demand of pressure to facilitate the discharge of the retentate. Processing, by recycling the retentate is therefore definitely limited by the viscosity and the corresponding pumpability of the slurry.

## 8. Washing and Purification Studies

The following section contains a general set up of the washing studies, used materials, the evaluation, and comparison of the washing studies. The principle process description, plant description and the explanation of the control system of the DynoTest are noted in chapter 4.2.

The aim of this work package was to investigate washing procedures with regard to general feasibility and subsequent implementation of washing and purification during filtration. NaCl was chosen as impurity, due to its high solubility in water. Ibuprofen was chosen as model substance, because of its hydrophobic properties so that less residual moisture was expected. Impurity measurement was done by using a conductivity sensor, mounted in the suspension buffer tank. Washing time and especially the amount of consumed washing agent was regarded and noted.

During the first study NaCl was washed out of the prepared suspension by introducing fresh buffer (inhere water) into the suspension buffer tank, while simultaneously removing the impurity-free retentate.

A further study was prepared by adding the washing agent step- or batch- wise.

### **Materials and Measurement Methods**

Sodium chloride (NaCl from Sigma Aldirch; Austria) was used to simulate impurities. At least suspensions were prepared as described in chapter 4.1., with an addition of 2 wt% of NaCl, which was previously dissolved in the respective mother liquid. Model substance was Ibuprofen.

The detection of impurities was done using a conductivity electrode (Knick Portamess 913 Cond with a ZU 6985 4 electrode sensor). The electrode was mounted inside the permeate collection container. Measurements were taken every 5 seconds and collected via the software parallel by Knick.



### First Washing experiment

During these studies the gained retentate was recycled. The schematic set up is shown in Figure 34.

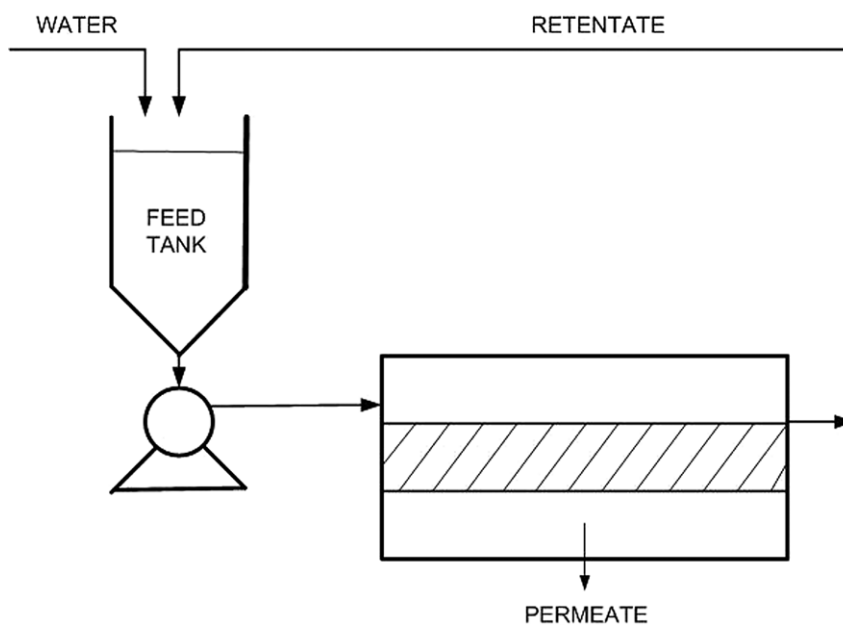


Figure 34: Process Description [24]

After the addition of NaCl the conductivity of the Ibuprofen-water-sodium pyrophosphate slurry increased from 10 up to  $\sim 45 \text{ mS}\cdot\text{cm}^{-1}$ . The addition of water was done incessantly and the amount of added water was equal to the amount of removed filtrate. The experiment was stopped as soon as the conductivity value of  $10 \text{ mS}\cdot\text{cm}^{-1}$  was reached. By this method, the volume of the fluid in the process chamber could be kept at a constant rate while the salt, dissolved in water, could pass through the filter and was washed out over time. The number of recycle steps, or loops, the time and the amount of wash water necessary to receive an impurity-free product, was noted.

Figure 35 shows the Conductivity Trajectory of the first washing experiments. The numbers of recycle steps are marked red. During each recycle step, 2 L of washing agent were consumed. As shown in the figure, at least 6 washing steps were needed to achieve a conductivity below  $10 \text{ mS}\cdot\text{cm}^{-1}$ . The overall amount of consumed wash water was 12 L.

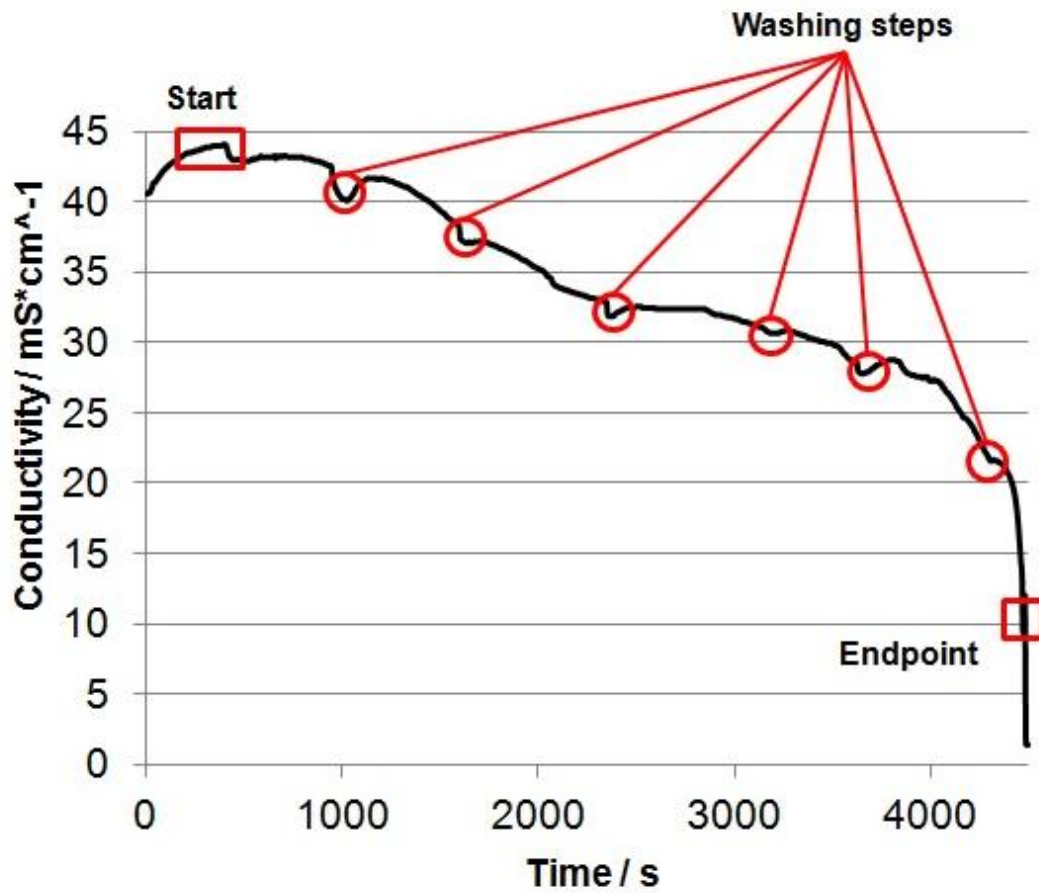


Figure 35: Conductivity Trajectory of Diafiltration

Rotor speed	1450	rpm
Feed rate (feed pump)	23	L/h
Feed rate (wash pump)	12	L/h
Suspension	15	%wt
Impurity	2	%wt

## Batch Diafiltration

Batch Diafiltration was done with the same suspension mixture and impurity concentration. In here the DynoTest was first used to concentrate the educts. While the filtrate was rejected, the gained retentate was collected and resuspended with washing agent. As a next step this water-product mixture was again delivered through the filtration unit. The number of resuspension of the retentate necessary to reach the desired conductivity value and the concentration steps were noted. In this method, the retentate concentration decreased as water agent was added and increased during concentration, so that buffer exchange wasn't that efficient.

Figure 36 shows the results of a washing test using the second setup with reslurry (Batch Filtraion). In this setup, the achieved amount of retentate was batch wise re-slurried. To do so, each filtration step was interrupted by collecting the retentate and the resuspension of this slurry with washing agent. At least 3 filtration steps were needed to receive values of conductivity below  $10 \text{ mS} \cdot \text{cm}^{-1}$ . The addition of wash water in-between each filtration step was 6 L, which resulted in an overall consumption of 12 L washing agent.

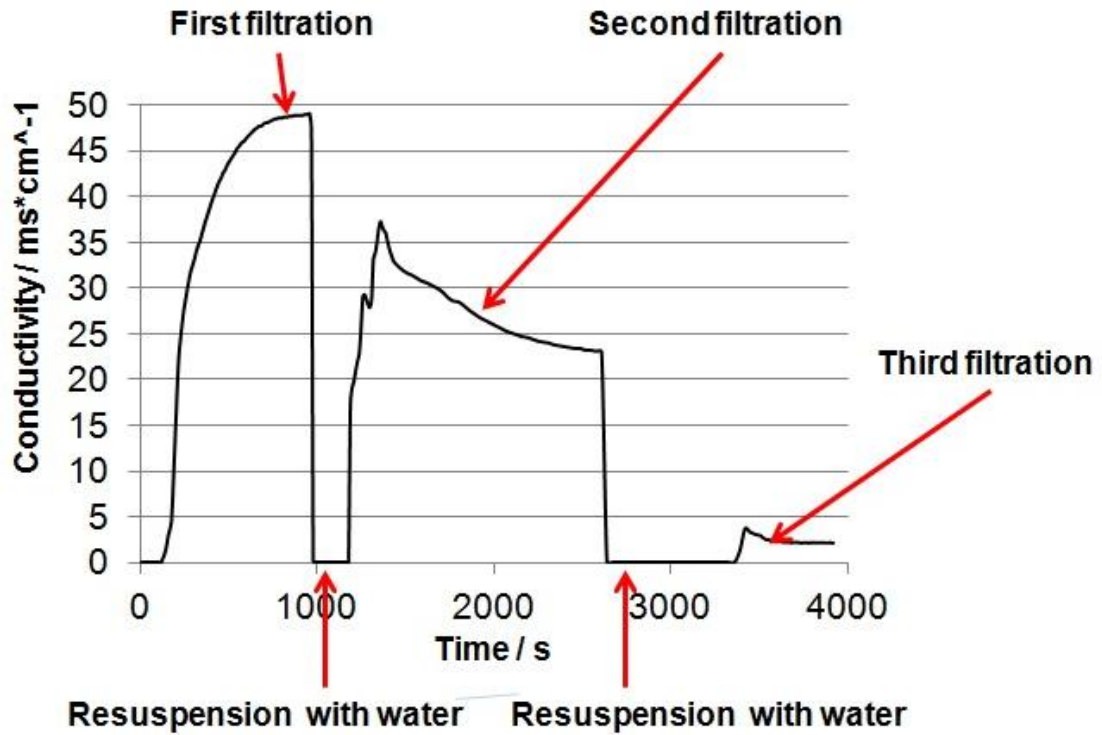


Figure 36: Conductivity Trajectory of Batch Filtration

Rotor speed	1450	rpm
Feed rate (feed pump)	23	L/h
Feed rate (wash pump)	12	L/h
Suspension	15	%wt
Impurity	2	%wt

## Conclusion

The amount of consumed wash water and the time span in both used set-ups are 12 L and ~ 4000 s.

Washing of the slurry can be done in two different ways, batch-wise or by diafiltration. As it is shown in Figure 35 and 36 both types needed the same amount of consumed wash water to achieve adequate purities.

Discharged permeate was recycled to purify the slurry during diafiltration, whereas fresh water was added during batch mode. This led at least to less working steps (stepwise addition of water) when operating under batch conditions. While it was necessary to recycle the permeate six times, only three working steps were necessary to purify the slurry in batch mode.

The permeate, a saturated Ibuprofen solution, might not be able to dissolve all the impurities within the slurry. This could be a result out of the different polarity and density than pure water has. On the other hand, fresh water might not only dissolve impurities, it also leads to an loss in amount of slurry, due to the resolution of Ibuprofen in water. This could be important if the substance to be purify is highly solute in water.

Nevertheless batch-wise purification of the slurry is the preferred way to achieve adequate purifications within adequate working steps. Since less working steps are required, also less modules are necessary within the pilot plant to achieve same purifications: Batch-wise purification is therefore the less cost intensive way.

## 9. Outlook and Conclusion

The challenge was to handle the pressure increase as a consequence out of the high flow resistances based on membrane pore size and surface characteristics of the API.

For subsequent studies following terms and conditions needed to be considered first:

- The optimal ratio for membrane pore size and particle size should be 1/10.
- Selection of the membrane should be based on the chemical properties of the mother liquid.
- Higher initial concentrations are required to achieve adequate results.

As stated in this thesis, hydrophobic membranes are more susceptible for membrane blocking. Hydrophilic membranes show a much better wettability for suspensions based on aqueous solutions. As a consequence flow resistances could be lowered.

The role of initial concentration could be ignored if the experimental set-up is changing. By recycling the retentate required values of residual moisture are mainly limited by the pumpability of the slurry.

Concluding it can be said, that there is a need of further investigation of the DynoTest. To do so experimental approaches have to be done referring to the material-membrane interaction. Materials differing in particle size distribution, particle shape and affinity to bind water should be tested out in accordance with the accessible residual moisture.

Resulting data could then be used for a better understanding and for defining the design space. Optimal operating conditions could only be established under executing further studies and evaluations.

---

**Notation**

$J$	permeate flow rate [ $\text{L h}^{-1} \text{m}^{-2}$ ]
$J_S$	convective transport of the fluid [ $\text{L h}^{-1} \text{m}^{-2}$ ]
$k$	mass transfer coefficient [ $\text{ms}^{-1}$ ]
$K$	Kozeny constant; depends on particle size, shape and porosity
$t$	time [s]
$V$	volume of filtrate [ $\text{m}^3$ ]
$m$	cake mass [kg]
$A$	face area [ $\text{m}^2$ ]
$N$	rotation speed [rpm]
$p$	pressure [Pa]
$p_c$	peripheral pressure [Pa]
$p_0$	pressure at center [Pa]
$p_f$	feed pressure (inlet pressure) [Pa]
$p_p$	pressure on the permeate side (outlet pressure) [Pa]
$\Delta p$	applied pressure [Pa]
$\rho_c$	density of the solid [ $\text{kgm}^{-3}$ ]
$\rho$	fluid density [ $\text{kgm}^{-3}$ ]
$\mu$	dynamic viscosity [Pa s]
$\nu$	kinematic viscosity [ $\text{m}^2 \text{s}^{-1}$ ]
$\alpha$	specific cake resistance [ $\text{m}^{-2}$ ]
$\varepsilon$	cake porosity [-]
$\delta$	thickness of the boundary layer [m]
$r$	radial distance [m]
$R$	disk radius [m]
$Re$	Reynolds number [-]
$R_m$	membrane resistance [ $\text{m}^{-1}$ ]
$R_t$	total filtration resistance [ $\text{m}^{-1}$ ]
$R_c$	cake resistance [ $\text{m}^{-1}$ ]
$R_{ads}$	resistance of solvent adsorbed onto the membrane surface [ $\text{m}^{-1}$ ]
$R_{cp}$	resistance of the concentration boundary layer [ $\text{m}^{-1}$ ]
$R_g$	resistance of concentrate at the membrane surface (gel layer) [ $\text{m}^{-1}$ ]
$C_B$	bulk concentration [kg/kg]
$C_G$	solid concentration on the membrane ("gel" concentration) [kg/kg]
$D$	diffusion coefficient [ $\text{cm}^2/\text{s}$ ]
$S_V^2$	mean particle surface area per unit volume [ $\text{m}^2/\text{L}$ ]
$c$	is the concentration of the solid in the suspension [kg/kg]
TMP	transmembrane pressure [Pa]
$R^2$	is the fraction of the variation of the response [-]
$Q^2$	is an index of the suitability of the chosen model [-]

---

## 10. List of Literature

- [1] K. PLUMB, "Continuous processing in the pharmaceutical industry; Changing the Mind Set," *IChemE*, pp. 730-738, June 2005.
- [2] L. Svarovsky, *Solid-Liquid Separation*, Oxford: Butterworth Heinemann, 2000.
- [3] M. Cheryan, *Ultrafiltration and Microfiltration Handbook*, Technomic Publising Company, Inc., 1998.
- [4] "Hyflux membranes," Hyflux Ltd, 2008. [Online]. Available: <http://www.hyfluxmembranes.com/microfiltration.html>. [Accessed 12 July 2012].
- [5] E. Staude, *Membran und Membran Prozesse*, Wiley VCH Verlag GmbH, 1992.
- [6] R. R. Thomas Melin, *Membranverfahren; Grundlagen der Modul- und Anlagenauslegung*, Aachen: Springer- Verlag Berlin Heidelberg, 2007.
- [7] K. Luckert, *Handbuch der mechanischen Fest-Flüssig-Trennung*, Vulkan-Verlag GmbH, 2004.
- [8] "KOCH MEMBRANE SYSTEMS," Koch Membrane Systems, Inc., 2011. [Online]. Available: <http://www.kochmembrane.com/PDFs/KMS-Membrane-Theory.aspx>. [Accessed 04.07.2012 Juli 2012].
- [9] M. Y. Jaffrin, "Dynamic shear- enhanced membrane filtration: A review of rotating disks, rotating membranes and vibrating systems," *Journal of Membrane Science*, pp. 7-25, 27 March 2008.
- [10] A. W. R. T. R. Rushton, *Solid- Liquid Filtration and Seperation Technology*, New York, NY: VCH Publishers, Inc., 1996.
- [11] Y. Y. V. C. A. G. F. Lee Nuang Sim, „Crossflow Sampler Modified Fouling Index Ultrafiltration (CFS-MFIUF)—An alternative Fouling Index," *Journal of Membrane Science*, p. 174–184, 2010.
- [12] J. H. M. R. N Mugnier, "Optimisation of a back-flush sequence for zeolite microfiltration," *Journal of Membrane Science*, p. 149–161, 10 August 2000.
- [13] J. A. Siegfried Ripperger, "Crossflow microfiltration – state of the art," *Separation and Purification Technology*, pp. 19-31, 01 January 2002.
- [14] „Bokela," BOKELA GmbH Karlsruhe, 2011. [Online]. Available: <http://www.bokela.de/de/technologien/cross-flow->



- filtration/membranfiltration/allgemeines.html. [Zugriff am 04 July 2012].
- [15] E. A. N. Endre Nagy, "Membrane mass transport by nanofiltration: Coupled effect of the polarization and membrane layers," *Journal of Membrane Science*, pp. 215-222, 15 February 2011.
- [16] F. M. White, Heat and mass transfer, ADDISON WESLEY Publishing Company Incorporated, 1988.
- [17] C. T. N. H. A.Y. Zahrim, „Coagulation with polymers for nanofiltration pre-treatment of highly concentrated dyes: A review," *Desalination*, pp. 1-16, 31 January 2011.
- [18] A.-S. Jiinsson, „Influence of shear rate on the flux during ultrafiltration of colloidal substances," *Journal of Membrane Science*, pp. 93-99, 22 Dezember 1992.
- [19] Malcolm Pirnie, Inc., Separation Processes, Inc., and The Cadmus Group, Inc., *MEMBRANE FILTRATION GUIDANCE MANUAL*, Cincinnati: United States Environmental Protection Agency, 2005.
- [20] MKS Umetrics AB, *User Guide to MODDE*, Sweden, Malmö, 2009.
- [21] INTERNATIONAL CONFERENCE ON HARMONISATION OF TECHNICAL, *PHARMACEUTICAL DEVELOPMENT Q8 (R2)*, INTERNATIONAL CONFERENCE ON HARMONISATION OF TECHNICAL, August 2009.
- [22] D. v. B. T. H. Karl Siebertz, Statistische Versuchsplanung, Design of Experiments (DoE), Berlin Heidelberg : Springer-Verlag, 2010.
- [23] A. S. R. & H. Winkle, "Quality by design for biopharmaceuticals," *nature biotechnology*, pp. 26-34, January 2009.
- [24] H. W. Irlmer, Dynamische Filtration mit keramischen Filtrationen, Vulkan-Verlag GmbH , 2001.
- [25] "New Logic Research," New Logic Research, Inc., 2012. [Online]. Available: <http://www.vsep.com/technology/index.html#3>. [Accessed 04 July 2012].
- [26] M. Y. J. A. L. P. P. Roger Bouzerar, "Concentration of ferric hydroxide suspensions in saline medium by dynamic cross-flow filtration," *Journal of Membrane Science*, pp. 111-123, 17 January 2000.
- [27] M. Y. J. L. D. P. P. Roger Bouzerar, "Influence of geometry and angular velocity on performance of a rotating disk filter," *AIChE Journal*, pp. 257-265, 16 April 2004.
- [28] L. D. M. Y. J. Roger Bouzerar, "Local permeate flux–shear–pressure relationships in a rotating disk microfiltration module: implications for global performance," *Journal of*

- 
- Membrane Science*, p. 127–141, 15 May 2000.
- [29] O. A. L. H. D. M. Y. J. Matthieu Frappart, „Treatment of dairy process waters modelled by diluted milk using dynamic nanofiltration with a rotating disk module,“ *Journal of Membrane Science*, pp. 465-472, 5 October 2006.
- [30] I. Borde and L. Avi, "Pneumatic and Flash Drying," in *Handbook of Industrial Drying*, Taylor & Francis, 2006, pp. 397-409.
- [31] G. Klinzing, F. Rizk, R. Marcus und L. Leung, *Pneumatic Conveying of Solids*, Springer, 2010.
- [32] W. Vauck and H. Müller, *Grundoperationen Chemischer Verfahrenstechnik*, Stuttgart: Deutscher Verlag für Grundstoffindustrie, 2000.
- [33] A. Apelblat, „Enthalpy of solution of oxalic, succinic, adipic, maleic, malic, tartaric, and citric acids, oxalic acid dihydrate, and citric acid monohydrate in water at 298.15 K,“ *Journal Chemical Thermodynamics*, Nr. 18, pp. 351-357, 1986.
- [34] K. Fischer, I. Shulgin, J. Rarey und J. Gmehling, „Vapor-liquid equilibria for the system water + tert.-pentanol at 4 temperatures,“ *Fluid Phase Equilibrium*, Nr. 120, pp. 143-165, 1996.
- [35] SPX Cooperation, "Anhydro Small Scale Spin Flash Dryer - Functional Description and Operator's Instructions," AI-01.08#03 ENG Version 1, 2012.
- [36] Verein Deutscher Ingenieure, „D Berechnungsmethoden für Stoffeigenschaften,“ in s *VDI Heat-Atlas*, Heidelberg, Springer, 2006.
- [37] Verein Deutscher Ingenieure, "E Wärmeleitung," in *VDI Heat-Atlas*, Berlin Heidelberg, Springer, 2006.
- [38] Y.-Y. Di, C.-T. Ye, Z.-C. Tan und G.-D. Zhang, „Low-temperature heat capacity and standard molar enthalpy of formation of crystalline (S)-(+)-Ibuprofen (C<sub>13</sub>H<sub>18</sub>O<sub>2</sub>)(S),“ *Indian Journal of Chemistry*, Nr. 46A, pp. 947-951, 2007.
- [39] APV Separations Product Group, "APV Dryer Handbook," West Sussex.
- [40] G. Reklaitis, J. Khinast and F. Muzzio, "Pharmaceutical engineering science - New approaches to pharmaceutical development and manufacturing," *Chemical Engineering Science*, vol. 65, no. 21, pp. iv-vii, 2010.
- [41] F. J. Muzzio, T. Shinbrot and B. J. Glasser, "Powder technology in the pharmaceutical industry: the need to catch up fast," *Powder Technology*, vol. 124, no. 1-2, pp. 1-7, 2002.
- [42] A.-G. Frank, "Anhydro Spin Flash Drying," Denmark, 2012.
-

- 
- [43] Europäisches Arzneibuch, 5. Ausgabe Hrsg., Bd. 1, Verlag Österreich, 2005.
- [44] G. Reich, "Near-infrared spectroscopy and imaging: Basic principles and pharmaceutical applications," *Advanced Drug Delivery Reviews*, no. 57, pp. 1109-1143, 2005.
- [45] S. C. Harris and D. S. Walker, "Quantitative Real-Time Monitoring of Dryer Effluent Using Fiber Optic Near-Infrared Spektroskopie," *Journal of Pharmaceutical Science*, vol. 89, no. 9, pp. 1180-1186, 2000.
- [46] G. X. Zhou, Z. Ge, J. Dorwart, B. Izzo, J. Kukura, G. Bicker und J. Wyvratt, „Determination and Differentiation of Surface and Bound Water in Drug Substances by Near Infrared Spectroscopy,“ *Journal of Pharmaceutical Science*, Bd. 92, Nr. 5, pp. 1058-1065, 2003.
- [47] Á. Kukovecz, T. Kanyó, Z. Kónya und I. Kiricsi, „Long-time low-impact ball milling of multi-wall carbon nanotubes,“ *Carbon*, Nr. 43, pp. 994-1000, 2005.
- [48] T. C. Alex, R. Kumar, A. J. Kailath, S. K. Roy und S. P. Mehrotra, „Physiochemical Changes During Mechanical Activation of Boehmite,“ Jamshedpur, 2010.
- [49] Umetrics Academy, Design of Experiment, USA.
- [50] D. S. Christen, Praxiswissen der chemischen Verfahrenstechnik, Berlin Heidelberg: Springer, 2005.
- [51] E. Berlin, P. G. Kliman, B. A. Anderson und M. J. Pallansch, „Calorimetric measurement of the heat of desorption of water vapor from amorphous and crystalline lactose,“ *Thermochimica Acta*, Bd. 2, pp. 143-152, 1970.
- [52] K. C. Patel und X. D. Chen, „Drying of aqueous lactose solutions in a single steam dryer,“ *Food and Bioproducts Processing*, Bd. 86, pp. 185-197, 2008.
- [53] EvaluatePharma, „World Preview 2018 - Embracing the Patent Cliff,“ EvaluatePharma, 2012.
- [54] J. L. Kukura und M. P. Thien, „Current Challenges and Opportunities in the Pharmaceutical Industry,“ in *s Chemical Engineering in the Pharmaceutical Industry*, New Jersey, Wiley, 2011.
- [55] T. J. Watson und R. Nosal, „Scientific Opportunities Through Quality by Design,“ in *s Chemical Engineering in the Pharmaceutical Industry - R&D to Manufacturing*, New Jersey, Wiley, 2011.
- [56] S. Murugesan, P. K. Sharma und J. E. Tabora, „Design of Filtration and Drying Operations,“ in *s Chemical Engineering in the Pharmaceutical Industry - R&D to Manufacturing*, New Jersey, Wiley, 2011.
-

- [57] A. Mersmann, M. Kind und J. Stichlmair, *Thermal Separation Technology*, Heidelberg: Springer, 2011.
- [58] A. M. Keech, „The Determination of Drying Kinetics and Equilibrium Characterisation at Low Moisture,“ University of Canterbury, Christchurch, 1997.
- [59] A. Reyes, G. Díaz und F.-H. Marquardt, „Analysis of Mechanically Agitated Fluid-Particle Contact Dryers,“ *Drying Technology*, Bd. 19, pp. 2235-2259, 2001.
- [60] J. Kim und G. Y. Han, „Effect of agitation on fluidization characteristics of fine particles in a fluidized bed,“ *Powder Technology*, Bd. 166, pp. 113-122, 2006.
- [61] S. Watano, N. Yeh und K. Miyanami, „Heat Transfer and the Mechanism of Drying in Agitation Fluidized Bed,“ *Chemical Pharmaceutical Bulletin*, Bd. 46, pp. 843-846, 1999.
- [62] D. Kunii und O. Levenspiel, *Fluidization Engineering*, Newton, USA: Butterworth-Heinemann, 1991.
- [63] A. Wadewitz und E. Specht, „Limit value of the Nusselt number for particles of different shape,“ *Int. J. Heat and Mass Transfer*, Bd. 44, pp. 967-975, 2001.
- [64] W. E. Ranz und W. R. Marshall, „Evaporation from Drops,“ *Chemical Engineering Progress*, Bd. 48, pp. 141-146, 1952.
- [65] L. R. Genskow, W. E. Beimesch, J. P. Hecht, I. Kemp, T. Langrish, C. Schwartzbach und L. F. Smith, „Chapter 12: Psychrometry, Evaporative Cooling, and Solids Drying,“ in s *Perry's Chemical Engineering Handbook 8th Edition*, McGraw-Hill, 2008.
- [66] S. Watano und K. Miyanami, „Image processing for on-line monitoring of granule size distribution and shape in fluidized bed granulation,“ *Powder Technology*, Bd. 83, pp. 55-60, 1995.

---

---